Contract NObsr-95349
Project Serial SF101-03-17
  Task 8139
TRACOR Project 002 025 04
Document Number 67-917-U

SUMMARY REPORT

EXPLORATORY DEVELOPMENT DOME STUDIES

Volume II

by

R. E. Douglass, K. B. Hamilton, and R. F. Pohler

Submitted to

Commander, Naval Ship Systems Command
Department of the Navy
Washington, D. C.   20360
Attention: Code 00V1E

9 October 1967

TRACOR

TRACOR 6500 TRACOR LANE. AUSTIN. TEXAS 78721

SUMMARY REPORT

EXPLORATORY DEVELOPMENT DOME STUDIES

Volume II

by

R. E. Douglass, K. B. Hamilton, and R. F. Pohler

Submitted to

Commander, Naval Ship Systems Command
Department of the Navy
Washington, D. C. 20360
Attention: Code 00V1E

9 October 1967

Approved: Submitted:

E. A. Tucker   *W. C. Moyer*

E. A. Tucker   W. C. Moyer
Director of Hydrospace Programs   Program Manager

TRACOR 6500 TRACOR LANE AUSTIN TEXAS 78721

TABLE OF CONTENTS

iii

TRACOR 6500 TRACOR LANE. AUSTIN. TEXAS 78721

LIST OF TABLES

DISCLAIMER NOTICE

THIS DOCUMENT IS BEST QUALITY PRACTICABLE. THE COPY FURNISHED TO DTIC CONTAINED A SIGNIFICANT NUMBER OF PAGES WHICH DO NOT REPRODUCE LEGIBLY.

OR are
Blank-pg?
that have
Been Removed

BEST AVAILABLE COPY

VOLUME II

1. INTRODUCTION

Volume II presents the detailed mathematical analyses used to obtain the results presented in Volume I*. The analytical models to be discussed represent mathematical descriptions of the dome-transducer acoustic interaction problem. This problem involves the simultaneous solution of the constitutive equations for the acoustic velocity field of a fluid and for the displacement field of a solid. A solution to this problem is impossible to obtain without assumptions which simplify the analysis, while still including the dominant physical mechanisms. The models to be discussed represent an attempt to analyze the general problem in terms of a simpler framework. The framework is constructed on assumptions which make the mathematics and computations tractable and at the same time yield information about the physical system. To a large extent, the purpose of analyzing the general problem from different sets of starting assumptions is to check the validity of the initial assumptions for a particular model. However, this approach has the advantage of isolating important mechanisms which are dominant in the behavior of a system.

The difficulties associated with obtaining a general solution fall into two categories. The first category is insufficient knowledge about the properties of the interacting system and its boundary conditions. The second category is lack of mathematical techniques for treatment of the general problem. Certain assumptions are usually made to obtain tractable models of radiating systems. These assumptions are as follows:

1. The system can be described by linearized constitutive equations for both the fluid and the solid.

2. The boundaries of the fluid in which the system is immersed are at infinity.

---

*The nonconcentric cylindrical dome has been treated in detail in Ref. [1] and will not be discussed here.

3. The fluid is homogeneous and inviscid.

4. The transient effects are neglected, i.e., the time dependence of all field quantities is given by $e^{-i\omega t}$ where ω is the angular frequency of oscillation and t is the time.

5. Velocity control is maintained on the transducer surface.

While the above assumptions yield a well-defined mathematical boundary value problem for the acoustic field, it is still impossible to solve this problem for arbitrary dome-transducer geometry and dome construction. Rather, it is necessary to devise a different mathematical model to study each part of the general problem. The assumptions which are employed most frequently in the models are described below.

In all the mathematical models except the one devised to study the effects of dome structure (see Section 7) the following assumption is made.

6. The dome material is homogeneous and has no supporting structure members.

It can be shown [2] that on the basis of Assumptions 1-6 the only geometrical shapes for which an eigenfunction solution for the dome motion can be obtained are two-dimensional circular cylinders, three-dimensional spherical shapes, and infinite plane surfaces. In order to exten' the description to geometries other than spheres or cylinders, it is necessary to make some additional assumptions about the dome. Thus in addition to the six stated assumptions, all models except the thick cylinder model of Section 7 are based on an additional assumption.

7. The dome thickness is small in comparison to an acoustic wavelength.

Assumption 7 allows the use of thin shell equations to describe the response of the dome.

2

To simplify the dome analysis even further, it is possible to use a result obtained from the thick dome model and from previous analyses [3]. At sonar transmit frequencies, the effect of a homogeneous dome is due entirely to its mass, for a limited range of dome thicknesses. This leads to the final assumption, employed only in the elliptic dome model.

8. The dome stiffness effects are negligible.

A further removal of geometrical restrictions to include a larger class of surfaces implies that eigenfunction expansion techniques are no longer applicable for analysis of the pressure field. It becomes necessary to use more general analytical techniques. The most promising mathematical technique for analysis of general surfaces is based on an integral formulation of the interaction problem. An integral formulation of the interaction problem, based on Assumptions 1-8, will be given, but the resulting algorithm has not yet been developed as fully as those previously mentioned.

From the previous discussion, it is evident that the mathematical models available for the interaction problem become less realistic in description of the dome as the geometrical restrictions are successively removed. In practice, computational techniques impose an additional constraint on the configurations which can be analyzed. The analyses in terms of eigenfunction expansions are more difficult for complicated geometries because the special functions involved are more difficult to compute. When the transducer and dome belong to different separable geometries, as in the elliptic dome model, it is necessary to calculate two different sets of special functions and establish a correspondence between them. The integral equation formulation is size-limited and, to analyze realistic size bodies, it is necessary to give up part of the method's shape versatility. Thus, even though mathematical techniques are available, in principle, to analyze a wide variety of geometrical configurations, the application of these techniques is still limited.

3

2. GENERAL METHODS - INTEGRAL EQUATION FORMULATION

The following four sections give a survey of the techniques developed for a numerical treatment of a restricted class of acoustic radiation problems.

2.1 INTEGRAL FORMULATION OF THE DOME-TRANSDUCER INTERACTION

The purpose of this section is to obtain a mathematical formulation of the dome-transducer interaction, subject to the eight assumptions stated in the Introduction.

The implication of these assumptions is that the acoustic pressure field can be determined by replacing the transducer and dome by equivalent source distributions on surfaces defined by the boundaries of the transducer and dome. (Because of Assumption 7 the dome can be replaced by one surface.) The pressure field is characterized in terms of the source strengths by the requirement that the field satisfy the inhomogeneous wave equation. The physical boundary conditions on the field at the surfaces then determine the source-strengths as solutions to a pair of coupled, integral equations.

The most general distribution of sources on a surface for which the field remains finite in the neighborhood of the surface is a superposition of simple (monopole) and dipole sources. The pressure field resulting from such a distribution on the transducer and dome surfaces can be written:

$$p(\vec{r}) = \int_{S_t} \left\{ \sigma_t(\vec{q}) \frac{\partial}{\partial n_q} G(\vec{r}|\vec{q}) + v_t(\vec{q}) G(\vec{r}|\vec{q}) \right\} dS(\vec{q})$$

$$+ \int_{S_d} \left\{ \sigma_d(\vec{q}) \frac{\partial}{\partial n_q} G(\vec{r}|\vec{q}) + v_d(\vec{q}) G(\vec{r}|\vec{q}) \right\} dS(\vec{q}) \quad , \quad (2.1\text{-}1)$$

4

where

$$G(\vec{r}|\vec{q}) = \frac{1}{4\pi} \frac{e^{ik|\vec{r}-\vec{q}|}}{|\vec{r}-\vec{q}|} \quad . \qquad (2.1\text{-}2)$$

In (2.1-1), $\vec{r}$ denotes an arbitrary point in the fluid medium, and $p(\vec{r})$ is the pressure at that point. The subscripts, d and t, denote respectively quantities associated with the dome and the transducer surfaces. The variable, $\vec{q}$, denotes an arbitrary point on either surface. The operator $\frac{\partial}{\partial n_q}$ applied to $G(\vec{r}|\vec{q})$ denotes the outward (toward the farfield) normal derivative with respect to the source coordinate. $\Psi(\vec{q})$ is the strength of the simple source distribution and φ is the strength of the dipole source distribution at the point $\vec{q}$ on the relevant surface. The choice of the source function G in (2.1-2) is based on the condition that the pressure field, p, satisfy the Sommerfeld radiation condition at infinity. (The time dependence is assumed to be given by the factor $e^{-i\omega t}$ and this factor is suppressed in all equations.) The wave number, k, in (2.1-2) is the ratio of the angular time-harmonic frequency and the sonic speed of the fluid.

In (2.1-1), the pressure field exterior to the transducer is expressed in terms of four unknown source distributions which must be determined from the given boundary conditions. In general both the field, $p(\vec{r})$, and its normal derivative experience jump discontinuities across the surfaces S_t and S_d. The jump discontinuity of a field variable, $f(\vec{r})$, across an arbitrary surface, S, is defined by the relation:

$$[[f]]_S = \lim_{\zeta \to 0^+} [f(\vec{q} + \vec{n}\zeta) - f(\vec{q} - \vec{n}\zeta)] , \qquad (2.1\text{-}3)$$

where $\vec{q}$ is an arbitrary point on S, and $\vec{n}$ is the normal to S at $\vec{q}$ pointing into the farfield. By making use of the singular properties of G it can be shown that

5

$$[[p]]_{S_t} = \tau_t(\vec{q}) \quad , \quad [[\vec{n} \cdot \nabla p]]_{S_t} = - \psi_t(\vec{q}) \quad ,$$

$$\tag{2.1-4}$$

$$[[p]]_{S_d} = \tau_d(\vec{q}) \quad , \quad [[\vec{n} \cdot \nabla p]]_{S_d} = - \psi_d(\vec{q}) \quad ,$$

and the jump discontinuity across any other closed surface is identically zero. The relations (2.1-4) hold at every point on the surfaces for which the principal curvatures are continuous. Use of Assumption 7 and the fact that the normal particle velocity, v_n, of the fluid is equal to that of the dome implies that

$$[[v]]_{S_d} = \frac{1}{i\omega\rho} [[\vec{n} \cdot \nabla p]]_{S_d} = 0 \quad , \tag{2.1-5}$$

where ω is the angular frequency of the time-harmonic oscillation, and ρ is the fluid density. Thus from (2.1-4) and (2.1-5),

$$\psi_d = 0 \quad . \tag{2.1-6}$$

Assumption 8 and Newton's law applied to the dome implies,

$$[[p]]_{S_d} = -i\omega\sigma N_d \quad , \tag{2.1-7}$$

where N_d is the normal velocity of the dome and σ is the surface density of the dome. Thus from (2.1-4)

$$\varphi_d = - i\omega\sigma N_d \quad , \tag{2.1-8}$$

$$\left[\vec{n} \cdot \nabla p\right]_{S_d} = i\omega\rho N_d(\vec{q}) \quad . \tag{2.1-9}$$

6

Equation (2.1-8) gives the physical interpretation of the dipole source distribution on the surface of the dome.

It still remains to determine the source distributions on the surface of the transducer. There is some degree of arbitrariness in the determination of these distributions because the region interior to the dome is not a region of physical interest. The physical boundary condition which must be satisfied on S_t is that determined by Assumption 5, i.e.,

$$\lim_{\zeta \to 0^+} \vec{n}_t \cdot \nabla p(\vec{q}_t + \vec{n}_t \zeta) = i\omega o \, N_t(\vec{q}_t) \, , \qquad (2.1\text{-}10)$$

where N_t is the specified, normal component of the velocity of the transducer, and $\vec{q}_t$ is an arbitrary point on the transducer surface, the surface curvature being continuous at that point.

This condition, (2.1-10), is not sufficient to determine the source distributions ω_t and ν_t uniquely, since according to (2.1-4) they are determined from the jump discontinuities of the pressure and the normal derivative at the transducer surface. Since the solution for the pressure field interior to the transducer is not of physical interest, it can be chosen to be any arbitrary solution to the time-independent wave equation. Once this arbitrary solution has been specified, the solution in the region of physical interest is determined from (2.1-10).

One of two choices is usually made for the arbitrary interior solution. The Helmholtz representation, used here, is obtained by requiring the interior solution to vanish identically. Using this condition and the relations (2.1-3) and (2.1-10) in (2.1-4) one obtains

$$\varphi_t(\vec{q}_t) = \lim_{\xi \to 0^+} p(\vec{q}_t + \vec{n}_t \xi) \, , \qquad (2.1\text{-}11)$$

7

and

$$\tau_t(\vec{q}_t) = -i\omega\ N_t(\vec{q}_t)\ ,\qquad\qquad (2.1\text{-}12)$$

where $\vec{q}_t$ represents an arbitrary point on the transducer surface. Thus, in this representation, the strength of the dipole source distribution has the physical interpretation of the surface pressure, and the strength of the simple source distribution is proportional to the transducer normal velocity, i.e., the normal component of the fluid velocity at the surface of the transducer.

The other convention which is in common use and which is called the "method of sources" is obtained by continuing the solution for the external pressure field into the interior of the transducer region with no discontinuity in value, i.e.,

$$[[p]]_{S_t} = 0\ .$$

Thus from (2.1-4), the above relation implies $\varphi_t = 0$. This amounts to the statement that the effect on the external fluid of the transducer is representable by a distribution of simple (monopole) sources. The strength, τ_t, of these sources does not have a direct physical interpretation. Mathematically, this distribution, from (2.1-4), can be interpreted as the discontinuity in the normal fluid particle velocity which must exist across the sur-- face S_t in order that the pressure field satisfy the wave equation at all points of space, except S_t, be continuous at all points of space, and have a specified normal derivative on one side of the surface. For rapidly varying velocity distributions, the Helmholtz representation seems preferable for computation, hence (2.1-11) and (2.1-12) will be employed. Making use of these relations and also (2.1-6) and (2.1-8) one obtains the relation

8

$$p(\vec{r}) = \int_{S_t} \left[p(\vec{q}) \frac{\partial}{\partial n_q} G(\vec{r}|\vec{q}) - i\omega\rho\, N_t(\vec{q})\, G(\vec{r}|\vec{q}) \right] dS$$

$$- i\omega \int_{S_d} \sigma(\vec{q})\, N_d(\vec{q}) \frac{\partial}{\partial n_q} G(\vec{r}|\vec{q})\, dS , \qquad (2.1\text{-}13)$$

in which the transducer surface pressure, $p(\vec{q})$, and the dome normal velocity, $N_d(\vec{q})$ are unknown. These quantities are determined from two coupled, integral equations obtained from (2.1-13). One integral equation is obtained by allowing the field point to approach the surface, S_t, from the farfield side. Taking account of the fact that near the singular point the dipole term behaves like the solid angle subtended at the field point by the surface, one obtains in the limit

$$p(\vec{q}_t) = \frac{p(\vec{q}_t)}{2} + {}^{*}\!\!\int_{S_t} \left[p(\vec{q}) \frac{\partial}{\partial n_q} G(\vec{q}_t|\vec{q}) - i\omega\rho\, N_t(\vec{q})\, G(\vec{q}_t|\vec{q}) \right] dS$$

$$- i\omega \int_{S_d} \sigma(\vec{q})\, N_d(\vec{q}) \frac{\partial}{\partial n_q} G(\vec{q}_t|\vec{q})\, dS . \qquad (2.1\text{-}14)$$

The asterisk on the integral means that the integral is the limit of a sequence of integrals obtained by excluding the singular point with surface patches whose areas tend to zero. The remaining integral equation is obtained by taking the limiting value of the normal component of the gradient of (2.1-13) as the field point approaches the dome from either side.

Making use of the relation (2.1-9) one obtains on performing the limiting process that

$$N_d(\vec{q}_d) = \frac{1}{i\omega\rho} \int_{S_t} \left[p(\vec{q}) \frac{\partial^2}{\partial n_d \partial n_q} G(\vec{q}_d|\vec{q}) - i\omega\rho\, N_t(\vec{q}) \frac{\partial}{\partial n_d} G(\vec{q}_d|\vec{q}) \right] dS$$

$$- \frac{1}{\rho} \int_{S_d} \sigma(\vec{q})\, N_d(\vec{q}) \frac{\partial^2}{\partial n_d \partial n_q} G(\vec{q}_d|\vec{q})\, dS . \qquad (2.1\text{-}15)$$

9

The relations (2.1-14) and (2.1-15) constitute a set of two, coupled, Fredholm integral equations which determine the transducer surface pressure and the normal velocity of the dome. The computational procedures used to solve these equations are the same as those used to treat a radiation problem with no dome. However, in this case it is necessary to subdivide both the transducer surface and the dome surface to obtain a set of algebraic equations which approximate the integral equations. From a computational point of view the only details which are new to the interaction problem are involved in establishing quadrature formulae for the kernels associated with the dome normal velocity. The kernel multiplying N_d in (2.1-14) is not singular on the dome surface and hence it is easy to treat numerically. (The same is true for the kernels associated with S_t in (2.1-15). Moreover the numerical details associated with the kernels defined on S_t have been discussed at length in the literature.) On the other hand, the kernel involving N_d in (2.1-15) needs to be defined more precisely in order that it have meaning, and this is the remaining detail which needs to be discussed in this section.

The last term on the right hand side of Eq. (2.1-15) is of the form

$$I(\vec{q}) = \int_S \psi(\vec{q}\,') \frac{\partial^2}{\partial n \partial n'} G(\vec{q}|\vec{q}\,') \, dS(\vec{q}\,') \qquad (2.1\text{-}16)$$

where S is a closed surface with a continuously turning tangent plane at every point and $\vec{q}$, $\vec{q}\,'$ are points on this surface. The function, $\psi(\vec{q})$ is a continuous and differentiable function of the surface coordinates and G is defined in (2.1-2). In the context used above, the integral on the right side of (2.1-16) is defined to be:

10

$$I(\vec{q}) = \lim_{\varsigma \to 0} \left\{ \vec{n} \cdot \nabla \int_S \psi(\vec{q}') \frac{\partial}{\partial n'} G(\vec{q} + \vec{n}\varsigma | \vec{q}') \, dS(\vec{q}') \right\}, \quad (2.1\text{-}17)$$

where $\vec{n}$ is the normal to S at $\vec{q}$. To analyze this limit it is convenient to introduce the source function for Laplace's equation:

$$G_o(\vec{r}|\vec{q}) = \frac{1}{4\pi} \frac{1}{|\vec{r} - \vec{q}|} \quad . \quad (2.1\text{-}18)$$

Consider the function:

$$F(\vec{r}) = \int_S \frac{\partial}{\partial n'} G_o(\vec{r}|\vec{q}') \, dS(\vec{q}') , \quad (2.1\text{-}19)$$

where S is the same surface which defined $I(\vec{q})$. Mathematically, $F(\vec{r})$ is $\frac{1}{4\pi}$ times the solid angle subtended at $\vec{r}$ by the surface S, and from the divergence theorem it follows that

$$F(\vec{r}) = \begin{cases} 1, & \vec{r} \text{ inside } S \\ \frac{1}{2}, & \vec{r} \text{ on } S \\ 0, & \vec{r} \text{ outside } S \end{cases} \quad (2.1\text{-}20)$$

Thus from (2.1-20) it follows that

$$\nabla F(\vec{q} + \vec{n}\varsigma) = 0, \quad \varsigma \neq 0 . \quad (2.1\text{-}21)$$

This means that adding any multiple of $F(\vec{r})$ to the right side of (2.1-17) will not affect the limit, hence on multiplying (2.1-19) by $-\psi(\vec{q})$ and adding the result to (2.1-17) one obtains

$$I(\vec{q}) = \lim_{\varsigma \to 0} \left\{ \vec{n} \cdot \nabla \int_S [\psi(q') \frac{\partial}{\partial n'} G(\vec{q} + \vec{n}\varsigma | \vec{q}') - \psi(\vec{q}) \frac{\partial}{\partial n'} G_o(\vec{q} + \vec{n}\varsigma | \vec{q}')] \, dS \right\} ,$$

11

or

$$I(\vec{q}) = \pm(\vec{q}) \lim_{\zeta \to 0} \int_S \frac{\partial^2}{\partial n \partial n'} [G(\vec{q} + \vec{n}\zeta | \vec{q}') - G_o(\vec{q} + \vec{n}\zeta | \vec{q}')] \, dS$$

$$+ \lim_{\zeta \to 0} \left\{ \int_S [\psi(\vec{q}') - \psi(\vec{q})] \frac{\partial^2}{\partial n \partial n'} G(\vec{q} + \vec{n}\zeta | \vec{q}') \, dS(\vec{q}') \right\} \; .$$

$$(2.1\text{-}22)$$

To evaluate the first limit on the right side of (2.1-22) consider the vector function

$$\vec{J}(\vec{r}) = \nabla \int_S \frac{\partial}{\partial n_q} [G(\vec{r} | \vec{q}) - G_o(\vec{r} | \vec{q})] \, dS \; , \qquad (2.1\text{-}23)$$

where $\vec{r}$ is not on S. The method of evaluation of the right side of (2.1-23) depends on whether $\vec{r}$ is exterior or interior to S although the final result is independent of that fact. Assume $\vec{r}$ is the interior to S and consider the region of space enclosed by S and the surfaces $\overline{S}$ of a small sphere centered at that point $\vec{r}$. In this region

$$\nabla'^2 [G(\vec{r} | \vec{r}') - G_o(\vec{r} | \vec{r}')] = -k^2 \, G(\vec{r} | \vec{r}') \quad . \quad (2.1\text{-}24)$$

Integrating (2.1-24) over the region bounded by S and $\overline{S}$, employing the divergence theorem, and showing that the contribution over $\overline{S}$ vanishes as the sphere excluding $\vec{r}$ tends to zero, one obtains

$$\int_S \frac{\partial}{\partial n_q} [G(\vec{r} | \vec{q}) - G_o(\vec{r} | \vec{q})] \, dS = -k^2 \int_V G(\vec{r} | \vec{r}') \, dV(\vec{r}') \; .$$

$$(2.1\text{-}25)$$

12

Thus from (2.1-23)

$$\vec{J}(\vec{r}) = - k^2 \nabla \int_V G(\vec{r}|\vec{r}') \, dV(\vec{r}') \; . \qquad (2.1-26)$$

Again, surround the point $\vec{r}$ by a small sphere centered at a fixed point $\vec{r}_o$ and break up the region of integration into two parts: the volume $\bar{V}$ included in the small sphere of radius "a" centered at $\vec{r}_o$ and the remaining volume $V-\bar{V}$. The integral over $\bar{V}$ can be performed analytically to yield

$$\nabla \int_{\bar{V}} G(\vec{r}|\vec{r}') \, dV(\vec{r}') = \frac{4\pi}{ik} (ka)^2 h_1(ka) \, j_1(k|\vec{r}-\vec{r}_o|) \frac{(\vec{r}-\vec{r}_o)}{|\vec{r}-\vec{r}_o|} \; ,$$

for $|\vec{r}-\vec{r}_o| < a$; where j_1 and h_1 are, respectively, spherical Bessel functions of the first and third kind.

For the remaining region, the gradient operation can be performed under the integral sign. Moreover, because of the form of G, the gradient with respect to field variables is the negative of the gradient with respect to the source variables. This fact and the divergence theorem allows the volume integral to be replaced by surface integrals over S and $\bar{S}$. Again the contribution over $\bar{S}$ vanishes as the radius of the sphere tends to zero and the limit of the analytic result above tends to zero with "a" when the limit is performed, keeping $|\vec{r}-\vec{r}_o| < a$. Thus the result is

$$\vec{J}(\vec{r}) = k^2 \oint \vec{n}(\vec{q}) \, G(\vec{r}|\vec{q}) \, dS(\vec{q}) \qquad (2.1-27)$$

The same result is obtained in a more straightforward fashion for $\vec{r}$ outside S. Thus from (2.1-23) and (2.1-29)

13

$$\lim_{\zeta \to o} \vec{n} \cdot \nabla \int_{S} \frac{\partial}{\partial n'} [G(\vec{q} + \vec{n}\zeta | \vec{q}') - G_o(\vec{q} + \vec{n}\zeta | \vec{q}')] \, dS_j$$

$$= k^2 \lim_{\zeta \to o} \int_{S} \vec{n}(\vec{q}) \cdot \vec{n}(\vec{q}') \, G(\vec{q} + \vec{n}\zeta | \vec{q}') \, dS(\vec{q}') \,,$$

$$= k^2 * \int_{S} \vec{n} \cdot \vec{n}' \, G(\vec{q} | \vec{q}') \, dS(\vec{q}') \,. \qquad (2.1\text{-}28)$$

The asterisk on the last integral in (2.1-28) has the same inter-
pretation as mentioned previously. The equality between the two
latter integrals in (2.1-28) is based on the result [4] that the
two limiting processes give identical results for a surface dis-
tribution of simple sources which is piecewise continuous. The
latter integral on the right side of (2.1-28) shows that the limit
of the integral on the left exists for all surfaces S having con-
tinuous curvature [4].

To evaluate the second limit on the right side of
(2.1-22) it is convenient to introduce the expression

$$\frac{\partial^2}{\partial n \partial n'} G(\vec{r} | \vec{r}') = k^2 \cos \gamma \cos \gamma' \, G - (R\frac{\partial G}{\partial R}) \frac{\partial^2}{\partial n \partial n'} \left(\frac{1}{R}\right) \qquad (2.1\text{-}29)$$

where

$$\vec{R} = \vec{r} - \vec{r}', \quad R = |\vec{r} - \vec{r}'| \,,$$

$$\cos \gamma = \frac{\vec{n} \cdot \vec{R}}{R} \,, \quad \cos v' = \frac{\vec{n}' \cdot \vec{R}}{R} \,.$$

The first term on the right hand side of (2.1-29) is proportional
to a simple source distribution, hence from classical results the

14

portion of the limit corresponding to this term exists. Moreover
the multiplicative factor of the mixed partial in the second term
is analytic in R. Thus an examination of the second limit reduces
to the consideration of an expression of the form

$$H(\vec{r}) = \vec{n} \cdot \vec{r} \int_S [\dot{v}(\vec{q}') - \dot{v}(\vec{q})] \frac{\partial}{\partial n_q} G_o(\vec{r}|\vec{q}') \, dS \,, \qquad (2.1\text{-}30)$$

where G_o is defined in (2.1-18).

According to classical results, if $\dot{v}(\vec{q}')$ is continuous
the jump discontinuity of H across S is zero. However, it is
necessary that $\dot{v}$ be twice differentiable with respect to the sur-
face coordinates in order that the limit exist on S. These mathe-
matical restrictions on $\dot{v}$ will always be satisfied by the source
density on a dome which is being driven by a pressure field and
thus one can conclude that both limits in (2.1-28) have meaning,
implying that the mathematical description of the physical prob-
lem is at least meaningful. On the other hand, the computation
of the limiting value of H in (2.1-30) is not as straightforward
because this limit is not, in general, equal to the limit of a
sequence of surface integrals which exclude the singular point.
For the conventional numerical approximation scheme which is
discussed in the literature, the knowledge that both limits exist
in (2.1-22) is sufficient to construct an algorithm for solution.
Namely, if the subdivision of the surfaces is made fine enough
so that, to the required degree of approximation, the variation
of the source strength is negligible over the individual surface
elements, then the contribution to the integral (2.1-30) over the
surface element for which the limit is difficult to perform is
identically zero for all values of $\vec{r}$, hence its limit is also
zero.

Thus it has been shown that the dome interaction prob-
lem, subject to the above assumptions, can be described by a set

15

of coupled integral equations which can be solved by the same techniques used to treat bare radiators.

2.2 HELMHOLTZ KERNELS FOR QUASI-SEPARABLE GEOMETRIES

In Section 2.1 it was shown that the integral equations for the source distributions involve kernels which are derived from a simple source function by differentiation with respect to a coordinate normal to the given surface. A numerical solution to these integral equations for general surfaces involves a large amount of computation because of their two-dimensional character. The purpose of this section is to discuss a restricted class of radiating surfaces for which the two-dimensional integral equation can be decomposed into a set of equivalent one-dimensional integral equations.

It is known from differential geometry, that the properties of a surface are determined by specifying its first and second ground forms:

$$d\vec{q} \cdot d\vec{q} = \sum_{\alpha=1}^{2} h_\alpha^2 (du_\alpha)^2 , \qquad (2.2\text{-}1)$$

$$2\vec{n} \cdot d\vec{q} = -\sum_{\alpha=1}^{2} h_\alpha^2 K_\alpha (du_\alpha)^2 . \qquad (2.2\text{-}2)$$

The relations (2.2-1) and (2.2-2) are the ground forms written in the principal coordinate system, and the K_α denote the principal curvatures. The presence of the negative sign in (2.2-2) arises from the convention that the curvature is considered positive if the surface bends away from the normal. Thus the curvature of a sphere is a positive constant. A general surface is defined by specifying the dependence of the scale factors, h_α, and the curvatures, K_α, as functions of the surface coordinates. From the

16

point of view of (2.2-1) and (2.2-2), the most simple surfaces to analyze are those for which the scale factors and the curvatures are independent of the surface coordinates. It turns out that the only surfaces for which these conditions are true are for infinite plane surfaces, and for these surfaces the method of inversion can be used to obtain a general solution of the wave equation.

The next class of surfaces in order of complexity are those for which the ground forms are independent of one surface coordinate, say the u_2 coordinate. It will be shown that the only classes of surfaces for which this is true are either (a) infinite cylinders with arbitrary cross section, or (b) axisymmetric bodies of revolution. For surfaces of these types, the dependence of the source kernels on the symmetry coordinate of the field point, u_2, and the source point, u_2', appears only in the combination $(u_2 - u_2')$, and it is this fact which allows the decomposition mentioned previously.

2.2.1   Quasi-Separable Surfaces

In the discussion, the orthonormal vectors tangent to the principal coordinate lines are denoted by $\vec{e}_\alpha$, the normal to the surface by $\vec{n}$, and differentiation with respect to surface coordinates by a subscript preceded by a comma. In terms of this notation, the mathematical definition of the surfaces under consideration is given by

$$h_{\alpha,2} = 0; \quad K_{\alpha,2} = 0 \quad . \qquad (2.2-3)$$

ln view of relations (2.2-3) and (2.2-1) there is no loss in generality in setting h_1 to unity. This gives u_1 the interpretation of being the arc length along the surface curves of constant values of u_2. Making use of (2.2-3), the fact that the u_α are principal coordinates, and the fact that $\vec{e}_1$, $\vec{e}_2$, $\vec{n}$ form an orthonormal triad, one obtains the partial differential equations:

17

$$\vec{\epsilon}_{1,1} = K_1 \vec{n}, \quad \vec{\epsilon}_{1,2} = h_{2,1} \vec{\epsilon}_2 , \tag{2.2-4a}$$

$$\vec{\epsilon}_{2,1} = 0, \quad \vec{\epsilon}_{2,2} = - h_2 K_2 \vec{n} - h_{2,1} \vec{\epsilon}_1 , \tag{2.2-4b}$$

$$\vec{n}_{,1} = K_1 \vec{\epsilon}_1, \quad \vec{n}_{,2} = h_2 K_2 \vec{\epsilon}_2 . \tag{2.2-4c}$$

The relations (2.2-4) can have a consistent solution only if the second mixed partial derivatives of the unit vectors are equal. In order that they be equal, the surface invariants must be related by the equations:

$$h_{2,11} = - h_2 K_2 K_1; \quad (h_2 K_2)_{,1} = h_{2,1} K_1 . \tag{2.2-5}$$

Solution of (2.2-5) yields

$$h_2 K_2 = C \sin \beta; \quad h_{2,1} = C \cos \beta , \tag{2.2-6a}$$

where

$$\beta_{,1} = K_1 , \tag{2.2-6b}$$

and C is an arbitrary constant. Making use of (2.2-6), the second of (2.2-4b) becomes

$$\vec{\epsilon}_{2,2} = -C[\vec{\epsilon}_1 \cos \beta + \vec{n} \sin \beta] . \tag{2.2-7}$$

This equation gives the interpretation of C and β; i.e., viewed as space curves, the u_2 curves have curvature C/h_2 and a normal which makes an angle $--\beta$ with $\vec{\varepsilon}_1$ in the plane of $\vec{\varepsilon}_1$ and $\vec{n}$. The binormal to these curves in a right-handed $\vec{\varepsilon}_1$, $\vec{\varepsilon}_2$, $\vec{n}$ system is

$$\vec{b}_2 = \vec{\varepsilon}_1 \sin \beta + \vec{n} \cos \beta \ , \qquad (2.2\text{-}8)$$

and the torsion is obtained as the magnitude of the derivative of $\vec{b}_2$. Using (2.2-4a), (2.2-4c) and (2.2-6a), one obtains

$$\vec{b}_{2,2} = \vec{\varepsilon}_{1,2} \sin \beta - \vec{n}_{1,2} \cos \beta = 0 \ .$$

Since the u_2 curves have vanishing torsion, they are plane curves. Moreover, from the first of (2.2-4b), the plane does not rotate as u_1 is varied. This means that there are two, fixed, orthogonal unit vectors, say $\vec{i}$ and $\vec{j}$, such that

$$\vec{\varepsilon}_2(u_1, u_2) = \vec{i} \cos \alpha + \vec{j} \sin \alpha \ , \qquad (2.2\text{-}9)$$

where α depends only on u_2. Also from (2.2-4) and (2.2-6) one obtains

$$\vec{\varepsilon}_{2,22} + C^2 \vec{\varepsilon}_2 = 0 \ . \qquad (2.2\text{-}10)$$

Thus from (2.2-9) and (2.2-10) one obtains

$$\alpha = C u_2 + \pi/2 \ ,$$

where choice of the arbitrary integration constant is made to conform to the usual definition of the spherical coordinate system. Hence

19

$$\vec{\varepsilon}_2 = -\vec{i} \sin C u_2 + \vec{j} \cos C u_2 \ . \tag{2.2-11}$$

Using (2.2-11) the expression for the binormal to the u_2 curves becomes

$$\vec{b}_2 = \vec{i} \times \vec{j} \equiv \vec{k} \ . \tag{2.2-12}$$

Also the first of relations (2.2-4a) and (2.2-4c) can be written

$$\frac{\partial \vec{\varepsilon}_1}{\partial \beta} = -\vec{n} \ , \quad \frac{\partial \vec{n}}{\partial \beta} = \vec{\varepsilon}_1 \ . \tag{2.2-13}$$

Using (2.2-8), (2.2-12) and (2.2-13) one obtains

$$\cos \beta \frac{\partial \vec{\varepsilon}_1}{\partial s} + \vec{\varepsilon}_1 \sin \beta = -\vec{k} \ , \tag{2.2-14}$$

which when solved yields

$$\vec{\varepsilon}_1 = -\vec{k} \sin \beta + \vec{\ell}(u_2) \cos \beta \ , \tag{2.2-15}$$

where, $\vec{\ell}$ is an arbitrary vector function of u_2. From (2.2-13)

$$\vec{n} = \vec{k} \cos \beta + \vec{\ell}(u_2) \sin \beta \ . \tag{2.2-16}$$

Relations (2.2-15), (2.2-16) and the fact that $\vec{\varepsilon}_1$, $\vec{\varepsilon}_2$, $\vec{n}$ are right-handed orthonormal vectors implies

$$\vec{\ell}(u_2) = \vec{i} \cos C u_2 + \vec{j} \sin C u_2 \ . \tag{2.2-17}$$

20

Hence the final solution for the unit vectors takes the form

$$\vec{n} = \vec{i} \sin \beta \cos C u_2 + \vec{j} \sin \beta \sin C u_2 + \vec{k} \cos \beta,$$

$$\vec{\varepsilon}_1 = \vec{i} \cos \beta \cos C u_2 + \vec{j} \cos \beta \sin C u_2 - \vec{k} \sin \beta,$$

$$\vec{\varepsilon}_2 = -\vec{i} \sin C u_2 + \vec{j} \cos C u_2 , \qquad\qquad (2.2\text{-}18)$$

where β and C are defined by (2.2-6). As mentioned previously C/h_2 is the curvature of the u_2 curves, $\vec{k}$ is the (constant) binormal to the u_2 curves. The interpretation of β follows from the first equation of (2.2-18) as being the angle between the normal to the surface and the binormal to the u_2 curves.

If C is set equal to unity in (2.2-18), one generates the class of axisymmetric bodies of revolution by interpreting u_2 to be the rotational coordinate. If C is set equal to zero, one obtains the class of infinite cylinders with the unit vector $\vec{j}$ defining the axis of the cylinder. Moreover the relations (2.2-5) show that when the surface invariants are independent of both surface coordinates, then both C and β must be set equal to zero, hence the relations (2.2-18) reduce to the equations of a plane.

An interpretation for general values of C is obtained by noting that the arc length along the u_2 curve is given by

$$s_2(u_1) = h_2 u_2$$

and, from above, the radius of curvature of the u_2 curve is given by

$$1/R_2 = C/h_2 .$$

Therefore, the last relation of (2.2-18) can be written as

$$\vec{\varepsilon}_2 = -\vec{i} \sin\left(\frac{s_2}{R_2}\right) + \vec{j} \cos\left(\frac{s_2}{R_2}\right) . \qquad (2.2\text{-}19)$$

Thus (2.2-19) shows that any non-zero value of C gives the same physical information as the value C = 1. In summary, it has been shown that the only surfaces for which (2.2-3) are satisfied are axisymmetric bodies, where infinite cylinders are a special case of axisymmetric bodies for which the symmetry axis moves off to infinity.

2.2.2   <u>Integral Equation for Axisymmetric Surfaces</u>

Having established the fact that all the surfaces defined by (2.2-3) are axisymmetric, it is convenient to introduce the rotational coordinate ω defined by the relation

$$\omega = C \, u_2 . \qquad (2.2\text{-}20)$$

Moreover it will be convenient to consider the fundamental triad as being the set $\vec{k}$, $\vec{\iota}$, $\vec{\varepsilon}_2$ which are the unit vectors of a cylindrical coordinate system. Equations (2.2-15), (2.2-16), (2.2-17) and (2.2-20) determine the relationships between this triad and the surface triad. In terms of the fundamental triad, the position vector to a point on the surface can be written

$$\vec{q}(u', \omega') = \vec{k} \, z'(u) + \vec{\iota}'(\varphi') \, \rho'(u') .$$

Also an arbitrary field point in space can be written

$$\vec{r} = \vec{k} \, z + \vec{\iota}(\varphi) \, \rho .$$

Hence

$$R = |\vec{r} - \vec{q}| = [(z - z')^2 + \rho^2 - 2\rho\rho' \cos(\varphi - \varphi') + \rho'^2]^{\frac{1}{2}} .$$
$$(2.2\text{-}21)$$

22

In (2.2-21) the primed coordinates refer to the source point and the unprimed coordinates refer to the field point. It should be kept in mind that z' and ρ' are parametrically related.

Making use of (2.2-16) and the expression for the gradient operator in cylindrical coordinates one obtains:

$$\frac{\partial}{\partial n'} = \vec{n}' \cdot \nabla' = \cos \beta' \frac{\partial}{\partial z'} + \sin \beta' \frac{\partial}{\partial \rho'} \quad , \qquad (2.2\text{-}22a)$$

$$\frac{\partial}{\partial n} = \vec{n} \cdot \nabla = \cos \beta \frac{\partial}{\partial z} + \sin \beta \frac{\partial}{\partial \rho} \quad . \qquad (2.2\text{-}22b)$$

Also, the differential surface area is

$$dS(\vec{q}') = h_1(u') \, \rho' \, du \, d\varphi \equiv \Omega(u') \, du' \, d\varphi'. \qquad (2.2\text{-}22c)$$

The special forms of relations (2.2-21) - (2.2-23) allow the decomposition of the integral representation for the pressure field given in Section 2.1, as will now be shown. For simplicity, the case of one radiating surface will be considered, but the analysis holds for any number of radiating surfaces as long as they are axisymmetric.

From Section 2.1, the most general form for the pressure field due to a distribution of simple and dipole sources on an axisymmetric surface is

$$p(\vec{r}) = \int du' \Omega(u') \frac{\partial}{\partial n'} \int_0^{2\pi} \Phi \, G(R) \, d\varphi' + \int_0^{2\pi} \psi \, G(R) \, d\varphi' \, ,$$

where $\qquad\qquad\qquad\qquad\qquad\qquad\qquad\qquad\qquad$ (2.2-24a)

$$G(R) = \frac{e^{ikR}}{4\pi R} \, , \qquad (2.2\text{-}24b)$$

23

and the remaining geometric quantities are defined in (2.2-21) –
(2.2-23). In writing (2.2-24), the special form of (2.2-22a) has
been used in order to interchange operations of integration and
differentiation. The source distributions, Φ and ψ, in (2.2-24a)
are functions of both u' and ω', and the condition that they be
single-values imposes the restriction that they be periodic in ω'
with period 2π. The most general function of the surface coordi-
nates which satisfies the periodicity stipulation is representable
in a Fourier series:

$$\Phi(u', \omega') = \sum_{m} \Phi_m(u') \, e^{im\omega'} \ . \tag{2.2-25}$$

Using (2.2-25), a corresponding representation for ψ, and the fact
that R is also a periodic function of ω', one obtains a Fourier
series representation for the pressure field:

$$p(\vec{r}) = \sum_{m} p_m(z, \rho) \, e^{im\omega} \ , \tag{2.2-26a}$$

where

$$p_m(z, \rho) = \int du' \ \Omega(u') \left[\Phi_m(u') \frac{\partial}{\partial n'} G_m + \psi_m(u') \, G_m \right] \ , \tag{2.2-26b}$$

$$G_m(z, \rho \mid z'(u') \, \rho'(u')) = \frac{1}{4\pi} \int_o^{2\pi} e^{im\alpha} \frac{e^{ikR(\alpha)}}{R(\alpha)} d\alpha \ , \tag{2.2-26c}$$

and

$$R(\alpha) = \left[(z - z')^2 + \rho^2 - 2\rho\rho' \cos \alpha + \rho'^2 \right]^{\frac{1}{2}} \ . \tag{2.2-26d}$$

24

The relations summarized in (2.2-26) characterize the pressure field in terms of a Fourier series, each coefficient p_m defined by an integral relation in terms of the coefficients of the source distributions. Due to the form of the normal component of the gradient operator given by (2.2-22b), the operation of taking the normal derivative of (2.2-26a) does not disturb the φ dependence. Also, it is to be noted that the kernels G_m are independent of the azimuth of the field point. Therefore, all of the statements made in Section 2.1 concerning the derivation of integral equations to determine the source distributions can be applied directly to each of the integral relations defined by (2.2-26c) to determine integral equations for the Fourier coefficients of the source distributions. Once they have been determined, the pressure field is obtained from (2.2-26a) and (2.2-26b). From the point of view of a numerical solution to the one-dimensional integral equations derived from (2.2-26b), the remaining detail to be considered is a method of calculating the source kernels.

The physical interpretation of the source kernels is obtained from the defining relation (2.2-26c). The function G_m is the pressure field at the point $\vec{r}$, due to a source distribution of constant amplitude, $\frac{1}{4}\pi$, and phase, $m\alpha$, on a ring of radius ρ' centered on the z-axis a distance z' above the origin. Except for the degenerate case for which the symmetry axis moves off to infinity, there is no known closed form expression for G_m, and one must be content with an infinite series or an integral representation for the G_m. However one would expect the singular part of the G_m to have the same behavior as for the degenerate case; hence it will be treated first.

2.2.3 Degenerate Case: Infinite Cylinders

To obtain the limiting form of the relations (2.2-25) and (2.2-26) as the radius ρ' of the ring gets large it is convenient to introduce the arc-length s' defined by

25

$$s' = \rho'\sigma' \quad , \tag{2.2-27}$$

and to refer the positions of the field point and the source point to a rectangular cartesian coordinate system with the origin on the ring and the y-axis tangent to the ring. The relationships between the original coordinates (ρ', θ') and (ρ, θ) and the new coordinates (x', y') and (x, y) are

$$x' + \rho' = \rho'\cos\theta' \quad , \quad x + \rho' = \rho\cos\theta \quad ,$$
$$y' = \rho'\sin\theta' \quad , \qquad y = \rho\sin\theta \quad . \tag{2.2-28}$$

Using (2.2-27) and passing to the limit of large ρ' shows that the source densities are represented by a Fourier integral:

$$\Phi(u', s') = \sum_m \rho'\,\Phi_m(u')\,e^{i\frac{m}{\rho'}s'}\,\Delta(\frac{m}{\rho'}) \rightarrow \int_{-\infty}^{\infty} \Phi_\sigma(u', \sigma)\,e^{i\sigma s'}\,d\sigma \quad , \tag{2.2-29a}$$

where $\sigma = \frac{m'}{\rho'}$, becomes a continuous variable in the limit of large values of ρ', and $\rho'\,\Phi_m(u') \rightarrow \Phi_\sigma(u', \sigma)$. Also for large values of ρ' it may be shown that

$$\frac{\partial}{\partial n'} \rightarrow \cos\beta\,\frac{\partial}{\partial z'} + \sin\beta\,\frac{\partial}{\partial x'} \quad . \tag{2.2-29b}$$

Moreover on using (2.2-27) and (2.2-28), and passing to the limit, one obtains:

$$G_\sigma(z, x \mid z'(u), x'(u)) \equiv \lim_{\rho'\to\infty} \rho'\,G_m$$

$$= \frac{1}{4\pi}\int_{-\infty}^{\infty} e^{i\sigma(y'-y)}\,\frac{e^{ik[(z-z')^2 + (x-x')^2 + (y-y')^2]^{\frac{1}{2}}}\,dy'}{[(z-z')^2 + (x-x')^2 + (y-y')^2]^{\frac{1}{2}}} \quad .$$

26

Introducing the variables

$$X = [(z - z')^2 + (x - x')^2]^{\frac{1}{2}} , \qquad (2.2\text{-}29c)$$

and

$$(y' - y) = X \sinh t ,$$

one obtains

$$G_\sigma(X) = \frac{1}{4\pi} \int_{-\infty}^{\infty} e^{i X(\sigma \sinh t + k \cosh t)} dt ,$$

or

$$G_\sigma(X) = \frac{i}{4} H_0(\sqrt{k^2 - \sigma^2} X) , \qquad (2.2\text{-}29d)$$

where H_0 is the zero order Hankel function of the first kind. Also, the limiting form of (2.2-26b) becomes

$$p_\sigma(z, x) = \int du' \, h_1(u') \left[\Phi_\sigma(u') \frac{\partial}{\partial n'} G_\sigma(X) + \psi_\sigma(u') G_\sigma(X) \right] . \qquad (2.2\text{-}29e)$$

The relations (2.2-29) are the defining equations for determining the pressure field on an infinite cylinder. The source kernels G_σ defined in (2.2-29d) are functions of a continuous parameter, σ, and of the magnitude, X, of the vector difference between field and source point projected onto the plane perpendicular to the axis of the cylinder. The closed form expression for G_σ is easy to calculate by well-known polynomial approximations; moreover the normal derivative of G_σ also has simple, approximate polynomial representations, and these representations provide a way of treating the singular parts and the regular parts of the kernels separately [5].

27

2.2.4   Series Representation of Source Kernels

Unfortunately, it has not been possible to find a representation of (2.2-26c) which has all of these desirable computational features. There are many representations for the G_m which can be obtained by expanding the simple source function in terms of the eigenfunctions of a separable coordinate system, but all of these expansions have the property that the real part is slowly convergent when the field point is close to the source point. The reason this happens is that each of the terms in the series is analytic when the field point and source are equal, and hence the series must diverge to represent the singularity. From the preceding analysis, one can ascertain that the dominant part of the singularity of the G_m should be the same as the zero order Hankel function, and, presumably, the singularity could be "subtracted" out of the series. However, the residual series would still have a branch point singularity, and ordinary numerical quadrature formulae applied to functions with branch points are not very accurate. In view of these considerations, it seems best to use an expansion in terms of functions each of which have a singularity of the same type as G_m itself so that the singular part can be treated in the same way as the degenerate case of an infinite cylinder.

An expansion which has the above feature and whose terms can be calculated from three term recursion relations is developed in the following manner.

Introduce the variables:

$$\eta = R(\pi) = [(z - z')^2 + (\rho + \rho')^2]^{\frac{1}{2}} , \qquad (2.2\text{-}30a)$$

$$R(\alpha) = \eta \cos \gamma(\alpha) , \qquad (2.2\text{-}30b)$$

28

and the identity

$$e^{ik\eta \cos \gamma} = \Gamma(\upsilon)(\frac{2}{k\eta})^{\upsilon} \sum_{n=0}^{\infty} (\upsilon + n)i^{n} J_{\upsilon + n}(k\eta) C_{n}^{(\upsilon)}(\cos \gamma) \quad , \tag{2.2-31}$$

to write (2.2-26c) in the form

$$G_{m} = \sum_{n=0}^{\infty} i^{n}(\frac{2}{k\eta})^{\upsilon} \frac{J_{\upsilon+n}(k\eta)}{\eta} T_{mn}^{(\upsilon)} \quad , \tag{2.2-32a}$$

where

$$T_{nm}^{(\upsilon)} = \frac{\Gamma(\upsilon)(\upsilon + n)}{4\pi} \int_{0}^{2\pi} e^{im\alpha} \frac{C_{n}^{(\upsilon)}(\cos \gamma(\alpha))}{\cos \gamma(\alpha)} d\alpha \quad . \tag{2.2-32b}$$

In (2.2-31), J_{υ} is the ordinary Bessel Function and C_{n}^{υ} is the Gegenbauer polynomial of degree n. The integral in (2.2-32b) can be evaluated by elementary methods by using the representation of the Gegenbauer polynomials in terms of hypergeometric functions:

$$C_{n}^{(\upsilon)}(\cos \gamma) = \frac{(2\upsilon)_{n}}{n!} \cos \gamma \, {}_{2}F_{1}(\frac{1-n}{2}, \frac{2\upsilon+n+1}{2}; \upsilon+\tfrac{1}{2}; \sin^{2} \gamma) \, . \tag{2.2-33}$$

From (2.2-26d) and (2.2-30) one obtains

$$\sin^{2} \gamma = v \cos^{2} \alpha/2 \quad , \tag{2.2-34a}$$

where

$$v = \frac{4\rho\rho'}{\eta^{2}} \quad . \tag{2.2-34b}$$

29

Substituting (2.2-33), (2.2-34a) into (2.2-32b), integrating term
by term, and making use of the identity

$$\frac{1}{2\pi} \int_0^{2\pi} e^{im\alpha} (\cos \alpha/2)^{2\ell} \, d\alpha = \begin{cases} 0 \, , & \ell < m \\ \frac{1}{2^{2\ell}} \binom{2\ell}{\ell + m} & \ell \geq m \, , \end{cases}$$

one obtains the result

$$T_{mn}^{(\upsilon)}(v) = \frac{\Gamma(\upsilon)(\upsilon+n)(2\upsilon)_n (\upsilon+\lambda_n+1)_m (-\lambda_n)_m}{2n! \, (\upsilon + \frac{1}{2})_m \, m!} \left(\frac{v}{4}\right)^m \, .$$

$$\cdot \,\, _3F_2(\upsilon+\lambda_n+m+1, \,\, -\lambda_n+m, \,\, m+\tfrac{1}{2}; \,\, \upsilon+m+\tfrac{1}{2}, \,\, 2m+1; \,\, v) \, ,$$

$$\text{(2.2-35)}$$

where

$$\lambda_n = \frac{n-1}{2} \, , \tag{2.2-36}$$

and the function on the right side of (2.2-35) is the generalized
hypergeometric function.

The relation (2.2-35) can also be written in the equi-
valent form

$$T_{n,m}^{(\upsilon)}(v) = \frac{\Gamma(\upsilon)(\upsilon+n)(2\upsilon)_n}{2n! \, m!} \, v^m \left(\frac{d}{dv}\right)^m {}_3F_2(\upsilon+\lambda_n+1, \,\, -\lambda_n, \,\, \tfrac{1}{2}; \,\, \upsilon+\tfrac{1}{2}, \,\, m+1; \,\, v) \, .$$

$$\text{(2.2-37)}$$

From (2.2-36), λ_n is an integer for odd values of n; hence the
hypergeometric function in (2.2-37) reduces to a finite polynomial.
Using this fact one obtains the result that

30

$$T^{(\cdot\cdot)}_{2k+1,m}(v) = 0 \quad \text{for} \quad k < m .$$

Also from (2.2-26c) and (2.2-32a) it is evident that the $T^{(\cdot\cdot)}_{nm}(v)$ for odd values of n represent the imaginary part of G_m, which is non-singular. On the other hand, the real part of G_m is singular at R = 0. From (2.2-26d), (2.2-30a) and (2.2-34b) the singular point corresponds to the value v = 1, and hence the singular nature of G_m must be reflected in the $T^{(v)}_{nm}(v)$ for even values of n and v = 1.

The singular properties of the generalized hypergeometric functions have not been studied as completely as those of the ordinary hypergeometric functions, and thus it is desirable to examine under what conditions the above relations for the $T^{(\cdot\cdot)}_{mn}$ reduce to the ordinary hypergeometric functions.

The fundamental identity given by (2.2-31) holds for all values of v which are not negative integers, and thus the value of v in the relations (2.2-31) through (2.2-38) can be chosen arbitrarily subject to the above restriction. On the other hand, the generalized hypergeometric function is reducible to a simpler form in two ways: (a) by choosing v such that a numerator parameter is equal to a denominator parameter, or (b) by moving the singular point to infinity to obtain a confluent form.

The first approach seems more straightforward, and from (2.2-37) it follows that the proper choice of v which is independent of n is the limit as v approaches zero through positive values. Making use of the relation

$$\lim_{v \to 0^+} \frac{\Gamma(v)(v+n)(2v)_n}{n!} = \begin{Bmatrix} 1, & n = 0 \\ 2, & n \neq 0 \end{Bmatrix} = \varepsilon_n ,$$

one obtains

31

$$T_{nm}(v) = \frac{\varepsilon_n}{2m!} v^m (\frac{d}{dv})^m \, {}_2F_1(\lambda_n+1, -\lambda_n; m+1; v) \, , \quad (2.2\text{-}38)$$

where the superscript $\nu = 0$ has been deleted, i.e., $T_{nm}(v) \equiv T_{nm}^{(0)}(v)$. The hypergeometric function on the right hand side of (2.2-38) is reducible to a finite combination of associated Legendre functions, i.e.,

$$T_{n,m}(v) = \frac{\varepsilon_n}{2(1+\lambda_n)_m \, (-\lambda_n)_m} v^m (\frac{d}{dv})^m \left[(\frac{1-v}{v})^{m/2} P_{\lambda_n}^m (1-2v) \right] ; \quad (2.2\text{-}39)$$

however, this relation is not useful for calculation except for $m = 0$ because the apparent square root branch point singularity does not exist in the T_{nm}. For $m = 0$, (2.2-39) reduces to

$$T_{n,0}(v) = \frac{\varepsilon_n}{2} P_{\lambda_n} (1-2v) \, , \quad (2.2\text{-}40)$$

where P_λ is the ordinary Legendre function. The relation (2.2-40) shows that $T_{n,0}$ are calculable from three-term recursion relations which, in view of (2.2-36) and the known recursion relations on Legendre functions, do not couple even and odd values of n. The functions $T_{n,0}$ for odd n are ordinary Legendre polynomials and for even n they are Legendre functions of half-integer order.

It is known that the three-term recursion relations for the Legendre functions are computationally stable with both increasing and decreasing values of the order if the magnitude of the argument is less than unity, so that the representation,

$$G_o = \sum_{n=o}^{\infty} \frac{\varepsilon_n}{2} i^n \frac{J_n(k\eta)}{\eta} P_{\frac{n-1}{2}} (1-2v) \, , \quad (2.2\text{-}41)$$

32

obtained by substituting (2.2-40) into (2.2-32a) is suitable for
computation. (From (2.2-34b), v = 0 corresponds to the case for
which either the source point or the field point is at one of
the poles of the axisymmetric body. If one uses the fact that
the Legendre functions of unit argument are unity, the relation
(2.2-41) can be summed by specializing (2.2-31) for $\nu \to o$ and
λ = o to get the familiar result. As mentioned, v = 1 corresponds
to the singular point so that the physical range of the argument
of the Legendre functions is between plus and minus unity.) More-
over, it will be shown that the singular part of (2.2-41) can be
isolated completely. The convergence of (2.2-41) is determined
by the argument of the Bessel functions, which are known to
decrease quite rapidly in magnitude after the order becomes,
roughly, twice the argument. Moreover, the Bessel functions
can be calculated by three-term recursion relations which are
stable in the direction of decreasing n.

To establish recursion relations satisfied by the
$T_{n,m}$ for arbitrary integral values of m, it is convenient to
rewrite (2.2-38) in the equivalent form

$$T_{nm}(v) = \frac{\varepsilon_n}{2} U_{\frac{n-1}{2}}^m (v) , \qquad (2.2\text{-}42a)$$

where

$$U_\lambda^m(v) = \frac{(\lambda+1)_m (-\lambda)_m v^m}{\Gamma(2m+1)} F(-\lambda+m, \lambda+m+1; 2m+1; v) , \quad (2.2\text{-}42b)$$

and the subscripts on the hypergeometric function have been
deleted since the discussion will be restricted to the ordinary
functions with two numerator parameters and one denominator param-
eter.

By making use of the recursive properties of the hyper-
geometric functions the following relation can be obtained:

$$A_1 \, F(a-1, \, b+1; \, c; \, v) + A_2 \, F(a, \, b; \, c; \, v) + A_3 \, F(a+1, \, b-1; \, c; \, v) = 0,$$

$$(2.2\text{-}43)$$

where

$$A_1 = b(c-a)(b-a-1),$$

$$A_2 = (b-a)[(2a-c)(b-a-1) - 2a(c-a-1) + (b-a+1)(b-a-1)v],$$

$$A_3 = a(c-b)(b-a+1).$$

Making use of (2.2-42b) and (2.2-43) one obtains the recursion
relation

$$\lambda \ (\lambda+1)^2-m^2]U^m_{\lambda+1} - (2\lambda+1)[m^2+\lambda(\lambda+1)(1-2v)]U^m_{\lambda} + (\lambda+1)(\lambda^2-m^2)U^m_{\lambda-1} = 0,$$

$$(2.2\text{-}44)$$

The relation (2.2-44) reduces to the recursion relation satisfied
by the Legendre functions of argument (1-2v) when m is set equal
to zero. Moreover, it has the same behavior as the relation for
Legendre functions for large values of λ, and, therefore, it has
the same stability properties. Thus the relations (2.2-44),
(2.2-42), (2.2-36) and (2.2-32a) (specialized to $\upsilon = 0$) define
the source kernels, G_m, by a series whose terms are calculable
from three-term recursion relations.

It still remains to isolate the singularity at $v = 1$.
To accomplish this, it is necessary to apply a linear transforma-
tion on the argument of the hypergeometric function in (2.2-42b).
The result is

$$U_\lambda^m(v) = \ln(1-v)\ V_\lambda^m(v)\ -\ W_\lambda^m(v)\ , \qquad (2.2\text{-}45a)$$

where

$$V_\lambda^m(v) = v^m\ \frac{\sin \pi\lambda}{\pi}\ F(-\lambda+m,\ \lambda+m+1;\ 1;\ 1-v)\ , \qquad (2.2\text{-}45b)$$

$$W_\lambda^m(v) = v^m\ \frac{\sin\pi\lambda}{\pi} \sum_{n=o}^{\infty} \frac{(-\lambda+m)_n(\lambda+m+1)_n}{(n!)^2}[\ 2\psi(n+1)-\psi(-\lambda+m+n)-\psi(\lambda+m+n+1)\ ](1-v)^n,$$

$$(2.2\text{-}45c)$$

and $\psi(z)$ is the Digamma Function.

Both $V_\lambda^m(v)$ and $W_\lambda^m(v)$ are analytic in the neighborhood of $v = 1$ according to the definitions (2.2-45b and c). Thus (2.2-45a) shows that the singularity of the U_λ^m is logarithmic. For integral values of λ, the U_λ^m are non-singular, as mentioned previously.

By applying (2.2-43) to (2.2-45b), it is easy to show that the $V_\lambda^m(v)$ satisfy the same recursion relations as the $U_\lambda^m(v)$, and since, according to (2.2-45a), the $W_\lambda^m(v)$ are a linear combination of the $U_\lambda^m(v)$ and the $V_\lambda^m(v)$, it follows that they also satisfy the same recursion relation. This result allows the singular part of the G_m to be separated quite easily from the non-singular part, and this feature will be used later in establishing numerical quadrature formulae.

Summarizing the relevant formulae, one finds that the G_m can be written (for the case $\upsilon = 0$ in (2.2-32)) as

$$G_m(z\rho\,|\,z'\rho') = \tfrac{1}{2}\sum_{n=o}^{\infty} \epsilon_n\ i^n\ \frac{J_n(k\eta)}{\eta}\ U_{\frac{n-1}{2}}^m(v)\ , \qquad (2.2\text{-}46)$$

where η and v are defined in (2.2-30a) and (2.2-34b) respectively. The functions, $U_\lambda^m(v)$, are determined by the recursion relation (2.2-44) and initializing values calculated from (2.2-42b). In

35

the neighborhood of the singularity, the representation of $U_\lambda^m(v)$ for non-integral values of λ is given by (2.2-45a) where the V_λ^m and the $W_\lambda^m(v)$ satisfy the same recursion relation (2.2-44) as the $U_\lambda^m(v)$, and the initializing values are obtained from (2.2-45b) and (2.2-45c).

Finally, it is necessary to consider the effect of applying the normal derivative operators defined in (2.2-22) to the representation of G_m given by (2.2-46). In terms of the independent variables η and v:

$$\frac{\partial}{\partial n'} = \frac{\partial \eta}{\partial n'} \frac{\partial}{\partial \eta} + \frac{\partial v}{\partial n'} \frac{\partial}{\partial v} \ , \qquad (2.2\text{-}47a)$$

$$\frac{\partial}{\partial n} = \frac{\partial \eta}{\partial n} \frac{\partial}{\partial \eta} + \frac{\partial v}{\partial n} \frac{\partial}{\partial v} \ . \qquad (2.2\text{-}47b)$$

The operator $\frac{\partial}{\partial \eta}$ applied to (2.2-46) gives a linear combination of Bessel functions, i.e.,

$$\frac{\partial}{\partial \eta} \left[\frac{-J_n(k\eta)}{\eta} \right] = \frac{k^2}{4n} \left[J_{n-2}(k\eta) - J_{n+2}(k\eta) \right] \ , \qquad (2.2\text{-}48)$$

so that the sum corresponding to applying this operator to (2.2-46) involves only Bessel functions and U-functions. However, in order to evaluate the normal derivatives it is necessary to find an expression for the derivative of the U-functions as a linear combination of functions of the same type. An examination of the normal derivatives of v shows that they can be written in the form:

$$\frac{\partial v}{\partial n'} = \frac{\sin \beta'}{\eta} - 2 \frac{(z'-z)\cos \beta' + (\rho'-\rho)\sin \beta'}{(z'-z)^2 + (\rho'-\rho)^2} \bigg] v(1-v) \ . \qquad (2.2\text{-}49a)$$

36

$$\frac{\partial v}{\partial n} = \left[\frac{\sin \beta}{\rho} - 2\frac{(z-z')\cos \beta + (\rho-\rho')\sin \beta}{(z-z')^2 + (\rho-\rho')^2}\right]v(1-v) \ . \quad (2.2\text{-}49\text{b})$$

The quantities in the brackets are finite everywhere the curvature is continuous on the surface of the radiator, so that for a smooth body it is only necessary to examine the effect of the operator $v(1-v)\frac{\partial}{\partial v}$ on the U-functions. (The motivation for specializing consideration to this operator rather than the derivative operator itself is seen from an examination of the special form of the kernel G_o given by (2.2-41). The derivative of a Legendre function has a higher order singularity than a Legendre function itself and hence cannot appear in the physical description. On the other hand, the operator $v(1-v)\frac{\partial}{\partial v}$ applied to a Legendre function gives a linear combination of Legendre functions. Finally, it may be noted that the right side of (2.2-49) vanishes for plane or spherical radiators when the field and source points are on the surface.)

Making use of (2.2-42b) and the properties of the hyper-geometric functions it may be shown that:

$$v(1-v)\frac{dU_\lambda^m}{dv} = \frac{1}{2\lambda}\left\{[m^2+\lambda^2(1-2v)]U_\lambda^m - (\lambda^2-m^2)U_{\lambda-1}^m\right\} \ . \quad (2.2\text{-}50)$$

The relations (2.2-47) through (2.2-50) when used in conjunction with (2.2-46) define the series representation for the dipole source kernels which appear in relations (2.2-26).

2.2.5   Summary

In summary, it has been shown that the class of axi-symmetric radiators are characterized by surface ground forms which are independent of one of the principal coordinates. The class of infinite cylinders is a degenerate case of axisymmetric bodies for which the symmetry axis is at infinity. For axisymmetric radiators, the two-dimensional integral representation of the pressure field can be decomposed into a set of one-dimensional

37

integral representations, and the source densities associated
with a particular axial mode can be obtained by solving a one-
dimensional integral equation. The resultant three-dimensional
pressure field is then obtained by a superposition of the contri-
butions from all the modes. The source kernels associated with a
particular mode have a logarithmic singularity and a prescription
for calculating these kernels has been given.

2.3   NUMERICAL SOLUTION OF ONE-DIMENSIONAL INTEGRAL EQUATIONS

In Section 2.2, it was shown that the Helmholtz integral
representation for the pressure field due to an axisymmetric
radiator can be decomposed into a set of modal representations,
defined by (2.2-26), which relate the modal amplitudes of the
pressure field to the corresponding amplitudes of the source
densities. The amplitude of a particular mode of the source
density is determined from a one-dimensional integral equation
which is derived from (2.2-26b) by allowing the field point to
approach the surface in the manner discussed in Section 2.1. The
general form of these integral equations can be written as

$$\varphi(u) = \int_a^b \sigma(u') \, K(u,u') \, du' - f(u) , \qquad (2.3\text{-}1)$$

where u is the variable characterizing points on the generating
curve of the radiator. The kernel, K, and the inhomogeneous
function, f(u), are determined by the methods outlined in Sections
2.1 and 2.2.

The problem to be considered here is that of replacing
the integral equation by a set of algebraic equations which are
obtained by a generalization of the usual methods. The basic
idea involved in this numerical approach is that the infinite
set of relations summarized by (2.3-1) is replaced by a finite
number of relations, i.e., the relation (2.3-1) is required to

38

hold only at discrete points (particular values of u) on the interval of integration. The fundamental question to be answered is: given a numerical solution to (2.3-1) which is obtained by requiring (2.3-1) to hold at N discrete points (referred to here as mesh points); how large must N be in order that the approximate solution is a good representation of the exact solution? It will be shown in the sequel that the approximate solution satisfies an integral equation of the same type as (2.3-1) except that the inhomogeneous term differs from that in (2.3-1) by a function which vanishes at all the mesh points. The details of an approximation scheme based on piecewise continuous interpolating functions will be presented and qualitative criteria for the choice of N will be given.

Let the mesh points be designated by a discrete index ranging from 1 to N and labeled in such a way that

$$u_{m+1} > u_m \ , \quad m = 1 \ldots N - 1 \ . \tag{2.3-2}$$

Moreover, let $\bar{\varphi}(u)$ be an approximate solution to (2.3-1) in the sense that it satisfies (2.3-1) at discrete mesh points, i.e.,

$$\bar{\varphi}_m = \int_a^b \bar{\varphi}(u') \ K(u_m, u') \ du' - f_m \ , \tag{2.3-3}$$

where

$$\bar{\varphi}_m \equiv \bar{\varphi}(u_m), \quad f_m = f(u_m) .$$

Define

$$\delta(u) = \bar{\varphi}(u) - \varphi(u) \ , \tag{2.3-4}$$

where φ is the exact solution to (2.3-1). Then on making use of (2.3-1) and (2.3-3) one finds that

$$\zeta(u_m) - \int_a^b \zeta(u') \, K(u_m,u') = 0 . \qquad (2.3\text{-}5)$$

Finally, if one defines the inhomogeneous function:

$$\gamma(u) = \zeta(u) - \int_a^b \zeta(u') \, K(u,u') \, du' , \qquad (2.3\text{-}6)$$

one finds on using (2.3-4) and (2.3-1) that

$$\gamma(u) = \int_a^b \gamma(u') \, K(u,u') \, du' - [f(u) - \epsilon(u)] . \qquad (2.3\text{-}7)$$

Moreover, from (2.3-5) and (2.3-6),

$$\gamma(u_m) = 0 . \qquad (2.3\text{-}8)$$

The relations (2.3-7) and (2.3-8) show the result stated previously, namely, that the approximate solution satisfies the integral equation with a modified inhomogeneous term. Moreover, (2.3-5) and (2.3-6) show that the difference between the approximate and exact solutions satisfies an integral equation of the same type, having an inhomogeneous term which vanishes at the mesh points.

The nature of the difference function, $\delta(u)$, depends on the particular type of approximation technique which is used to obtain the solution $\tilde{\zeta}(u)$. The discussion in this section will be limited to approximation schemes which are based on the use of piecewise continuous functions. Specifically, the set of piecewise functions which are to be discussed consist of polynomials which are constructed to interpolate the functional values at the mesh points.

The mathematical definition of the interpolating polynomials to be used is the following: Let u_j be an arbitrary

40

interior mesh point and define the midpoints of the segments adjacent to this mesh point by

$$a_j = (u_{j-1} + u_j)/2 \quad , \tag{2.3-9a}$$

$$b_j = (u_{j+1} + u_j)/2 \quad . \tag{2.3-9b}$$

Denote by $\bar{P}_j(u)$ the interpolating polynomial of degree 2K which is defined over the interval $a_j < u < b_j$. Then,

$$\bar{P}_j(u) \equiv \sum_{\ell=j-K}^{j+K} \bar{\phi}_\ell \frac{Q_j(u)}{(u-u_\ell) Q'_j(u_\ell)} \quad , \tag{2.3-10a}$$

where

$$Q_j(u) = \prod_{k=j-K}^{j+K} (u - u_k) \quad , \tag{2.3-10b}$$

and a prime on Q_j denotes differentiation with respect to u. The relation (2.3-10) is the Lagrangian interpolation formula of numerical analysis, and (2.3-10) is a restatement of the fact that

$$\bar{P}_j(u_k) = \bar{\phi}_k \quad , \quad k = j-K \ldots j+K \quad . \tag{2.3-11}$$

It is to be noted that even though the interpolating function reproduces the functional values at 2K+1 mesh points, its interval of definition extends only a half mesh point spacing on either side of the central mesh point u_j. Also, the definition (2.3-10) holds only for those mesh points for which $K < j < N-K$. The remaining mesh points must be treated somewhat differently.

41

Alternatively, one can define (2.3-3) to hold also for the remaining mesh points by extending the mesh past the physical range of the variable u and defining the values of φ in the non-physical range in some convenient manner. This approach amounts to making some statements about the derivatives of the function φ at the end points of the physical range of u. In most physical problems the end points of the interval correspond to special points for which additional information about the function is available, and hence can be used. A particular example of immediate interest is the integral equation for the source density on an infinite cylinder. For this case u parameterizes a closed curve, and the source density must be single valued. This implies that the source density should be extended into the non-physical region as a periodic function.

Generally, it will be assumed that the non-physical values of φ have been chosen in a manner consistent with the physical nature of the function φ and the parameter u, and (2.2-3) will be taken to hold for $1 \le j \le N$. Then, in terms of the set of piecewise continuous functions, $\bar{P}_j$, the approximating function can be written

$$\bar{\varphi}(u) = \sum_{j=1}^{N} U[(b_j - u)(u - a_j)] \bar{P}_j(u) , \qquad (2.3\text{-}12a)$$

where $U(t)$ is the Heaviside step function, i.e.,

$$U(t) = \begin{cases} 0 & t < 0 \\ \\ 1 & t > 0 \end{cases} \qquad (2.3\text{-}12b)$$

42

Making use of the fact that

$$\bar{P}_j(u_j) = \bar{\varphi}_j \quad , \tag{2.3-13}$$

and of the properties of the step function, it is easily verified that

$$\bar{\varphi}(u_m) = \bar{\varphi}_m \quad m = 1\ldots N \quad ; \tag{2.3-14}$$

hence $\bar{\varphi}(u)$ reproduces the functional values at all the mesh points. It is to be noted that (2.3-14) holds for any integrable function $\bar{P}_j(u)$ which is constrained by the single condition given by (2.3-13). A choice of the $\bar{P}_j(u)$ which is different from that of (2.3-10) can only affect the difference function, $\delta(u)$, defined by (2.3-14).

Substitution of (2.3-12) into (2.3-3) yields

$$\bar{\varphi}_m = \sum_{j=1}^{N} \int_{a_j}^{b_j} \bar{P}_j(u') \, K(u_m, u') \, du' - f_m \quad . \tag{2.3-15}$$

The relation (2.3-15) is valid for arbitrary integrable functions, and at this point one could proceed to derive a general set of algebraic equations for the $\bar{\varphi}_m$ by choosing an arbitrary set of functions $\bar{P}_j(u)$ which are normalized according to (2.3-13). The choice of interpolating polynomials is based on the fact that they are relatively complete and their choice does not unduly complicate the evaluation of the definite integrals. Thus on using (2.3-10) one obtains:

43

$$\bar{\varphi}_m = \sum_{j=1}^{N} \sum_{\ell=j-K}^{j+K} \bar{\varphi}_\ell \, K_{mj\ell} - f_m \, , \qquad (2.3\text{-}16a)$$

where the weighting factors are defined by:

$$K_{mj\ell} = \int_{a_j}^{b_j} K(u_m, u') \, \frac{Q_j(u')}{(u'-u_\ell) \, Q_j'(u_\ell)} \, du' \, . \qquad (2.3\text{-}16b)$$

To reduce (2.3-16a) to a determinate set of relations, it is necessary to give explicit forms to the $\bar{\varphi}_\ell$ whose indices are outside the range from 1 to N. For physical problems of interest here, the most general defining relation takes the form

$$\bar{\varphi}_{-\ell+1} = \sum_{k=1}^{N} A_{\ell k}^{(-)} \, \bar{\varphi}_k \quad \ell = 1 \ldots K \, , \qquad (2.3\text{-}17a)$$

$$\bar{\varphi}_{N+\ell} = \sum_{k=1}^{N} A_{\ell k}^{(+)} \, \bar{\varphi}_k \quad \ell = 1 \ldots K \, . \qquad (2.3\text{-}17b)$$

Making use of (2.3-17) in (2.3-16a) obtains:

$$\bar{\varphi}_m = \sum_{k=1}^{N} F_{mk} \, \bar{\varphi}_k - f_m \, , \qquad (2.3\text{-}18a)$$

where

$$F_{mk} = \sum_{n=J_1(k)}^{J_2(k)} K_{mnk} + \sum_{\ell=1}^{K} \left[A_{\ell k}^{(-)} \sum_{n=1}^{K-\ell+1} K_{mn,-\ell+1} + A_{\ell k}^{(+)} \sum_{n=\ell+N-K}^{N} K_{m,n,\ell+N} \right] \, , \qquad (2.3\text{-}18b)$$

44

and

$$J_1(k) = \max\,(1,\ k\text{-}K)\ ,\qquad\qquad (2.3\text{-}18c)$$

$$J_2(k) = \min\,(k\text{+}K,\ N)\ .\qquad\qquad (2.3\text{-}18d)$$

The solution of (2.3-18a) determines the approximate function at
the chosen mesh points. Once these values have been obtained,
the relations (2.3-17), (2.3-12), and (2.3-10) determine the solu-
tion at every point on the interval.

The next step involves establishing some criterion
to determine how accurately the approximate solution represents
the exact solution, $\varphi(u)$. Basically, there are three types of
errors introduced in obtaining a solution to (2.3-18a). The first
type of error results from attempting to model a continuous func-
tion by the quasi-continuous representation given by (2.3-12a).
The second type of error is introduced by the assumption that the
exact function φ is representable by a polynomial of degree 2K
in the interval $a_j < u < b_j$. The third type results from numerical
calculation of the matrix elements, F_{mk}, and the solution of the
algebraic system (2.3-18a). An error of the third type can, in
principle, be minimized by efficient numerical algorithms, as
will be discussed in the next section. It is to be noted that the
difference function, $\delta(u)$, defined by (2.3-4) accounts only for
errors of the first and second type.

It may be shown that errors of the first type vanish
identically at the mesh points if the kernel and the inhomogeneous
function satisfy certain restrictions. To see this, it is neces-
sary to substitute (2.3-12a) into the integral and compare the
result to the function $\bar{\varphi}(u)$; i.e., define

$$\bar{\mathfrak{I}}_1(u) = \int_a^b \bar{\mathfrak{I}}(u') \, K(u,u') \, d' - f(u) \; . \qquad (2.3\text{-}19)$$

Making use of (2.3-15) and (2.3-10) it follows that

$$\bar{P}_j(u) = \int_a^b \bar{\phi}(u')\bar{K}_j(u,u') \, du' - \bar{f}_j(u) \; , \qquad (2.3\text{-}20a)$$

$$\bar{K}_j(u,u') = \sum_{\ell=j-K}^{j+K} K(u_\ell,u') \, \frac{Q_j(u)}{(u-u_1) \, Q_j'(u_\ell)} \; , \qquad (2.3\text{-}20b)$$

$$\bar{f}_j(u) = \sum_{\ell=j-K}^{j+K} f(u_\ell) \, \frac{Q_j(u)}{(u-u_1) \, Q_j'(u_\ell)} \; . \qquad (2.3\text{-}20c)$$

Substitute (2.3-20a) into (2.3-12a) and subtract the result from (2.3-19) to obtain:

$$[\bar{\mathfrak{I}}_1(u) - \bar{\mathfrak{I}}(u)] = \int_a^b \bar{\mathfrak{I}}(u')[K(u,u') - \bar{K}(u,u')]du' - [f(u) - \bar{f}(u)] \; , \qquad (2.3\text{-}21a)$$

where

$$\bar{K}(u,u') = \sum_{j=1}^{N} U[(b_j-u)(u-a_j)] \, \bar{K}_j(u,u') \; , \qquad (2.3\text{-}21b)$$

and

$$\bar{f}(u) = \sum_{j=1}^{N} U[(b_j - u)(u - a_j)]\bar{f}_j(u) . \qquad (2.3\text{-}21c)$$

The relations (2.3-20) and (2.3-21) show that if the kernel and
the inhomogeneous function are bounded, then that part of the
difference function, $\delta(u)$, which is due to an approximation of
the first type, depends on the error introduced by representing
the u-dependence of the kernel and the inhomogeneous function by
an interpolating polynomial of degree 2K in the intervals $a_j < u <
b_j$. Moreover, these relations show that

$$\bar{\omega}_1(u_j) - \bar{\omega}(u_j) = 0 , j = 1\ldots N ; \qquad (2.3\text{-}22)$$

i.e., an error of the first type vanishes at the mesh points if
the kernel and inhomogeneous functions are bounded at the mesh
points. It turns out that (2.3-22) is also satisfied if the
kernel K is merely integrable. It is important to note, however,
that the relation (2.3-22) is not sufficient to insure that the
solution $\bar{\varphi}(u)$ is a good approximation to the exact function $\varphi(u)$
even at the mesh points. The reason this is true can be seen from
(2.3-21a). If the left hand side of (2.3-21a) is not a small
quantity at every point on the interval $a \le u \le b$, then the origi-
nal assumption about the variation of $\bar{\omega}$ has been violated and
hence the solution for the $\bar{\varphi}_m$ is not valid. Thus from (2.3-20)
and (2.3-21) it follows that a solution obtained by the above
scheme can be meaningful, only if the mesh points are spaced closely
enough that the interpolating polynomial used is of sufficiently
high degree to represent the variations of both the kernel and the
inhomogeneous function over the entire interval. This condition
insures that an error of the first type has a small effect on the
function at the mesh points.

It still remains to determine the effect of an error of the second type. In order to do this, it is necessary to examine the remainder term associated with a polynomial approximation of the type given by (2.3-10). A discussion of this problem is given in most texts on numerical analysis [6]. The result for a function which is differentiable can be written:

$$\varphi(u) = P_j(u) + \delta_j(u) \, , \, a_j < u < b_j \, , \qquad (2.3\text{-}23a)$$

where

$$\delta_j(u) = \frac{\varphi^{(2K+1)}(\xi)}{(2K+1)!} \, , \qquad (2.3\text{-}23b)$$

and where $P_j(u)$ is defined by (2.3-10) with the $\bar{\varphi}_1$ replaced by the φ_1; ξ is a point in the interval $u_{j-K} < \xi < u_{j+K}$; and the super-script on φ denotes the order of the derivative.

The relation (2.3-23b) shows that if the function has derivatives up to order 2K+1, then the error in a polynomial inter-polation vanishes at the mesh points. This means that in the absence of any weaker constraints, an approximation scheme using interpolating polynomials is limited to those integral equations which admit solutions that are differentiable up to order 2K+1.

An analysis of the perturbation effects of adding a term of the form of (2.3-23b) to (2.3-12a) requires further study. One qualitative statement which can be made here is based on the fact that the perturbing term given by (2.3-23b) is a polynomial of degree 2K+1. Thus, one could partially account for this term by increasing the degree of the interpolating function in (2.3-10) to 2K+2 by including K+1 adjacent mesh points on each side of the central mesh point. Then one could repeat the same arguments used to derive (2.3-20) and (2.3-21) to obtain analogous expressions, except that, in this case, the kernel and the inhomogeneous function

48

would be interpolated by polynomials of degree 2K+2. One would expect that if the kernel and the inhomogeneous function are reasonably well represented by an interpolating polynomial of degree 2K then the difference between the approximate solutions obtained using interpolating polynomials of degree 2K and 2K+2 should be small. Hence, it would appear that a mesh point distribution which is fine enough to interpolate the kernel and the inhomogeneous function with a polynomial of degree 2K is both necessary and sufficient to insure that an approximate solution based on an interpolating polynomial of the same degree is reasonably accurate.

When applied to the integral equation for pressure sources on a radiator, the above considerations imply that, for velocity distributions which are rapidly varying (e.g., discontinuous), the "Helmholtz" formulation is preferable to the "source" formulation since the inhomogeneous function of the Helmholtz formulation is more slowly varying than that for the source formulation.

2.4   EVALUATION OF THE MATRIX ELEMENTS

In Section 2.3, it was shown that the algebraic system of equations which define an approximate solution to a one-dimensional integral equation depend on a set of weighting factors of the kernel, defined by (2.3-16b). In Section 2.2 it was shown that the kernels associated with axisymmetric radiators have a logarithmic singularity, consequently ordinary quadrature formulae are inaccurate when used to evaluate the weighting factors near the singularity.

It will be shown in this section that the weighting factors are linear combinations of a set of quantities called moments of the kernel, and numerical quadrature formulae which account for the singular nature of the kernel will be given.

49

From Section 2.3, the definition of the weighting
factors is given by

$$K_{\ell mn} = \int_{a_m}^{b_m} K(u_\ell, u') \frac{Q_m(u')\, du'}{(u'-u_n)\, Q'_m(u_{r.})} \quad . \qquad (2.4\text{-}1)$$

From (2.3-10), the coefficient of the kernel under the integral
sign is a polynomial of degree 2K in the integration variable,
u'. Moreover, the relation

$$(u' - u_m)^k = \sum_{n=m-K}^{m+K} \frac{(u_n - u_m)^k\, Q_m(u')}{(u' - u_n)\, Q'_m(u_n)} \quad , \qquad (2.4\text{-}2)$$

is an identity for $0 \le k \le 2K$ and k integral. Thus on multiplying
(2.4-2) by $K(u_\ell, u')$, integrating, and using (2.4-1) one obtains

$$M_{\ell mk} = \sum_{n=m-K}^{m+K} (u_n - u_m)^k\, K_{\ell mn} , \quad k = 0, \ldots 2K \quad , \qquad (2.4\text{-}3)$$

where

$$M_{\ell mk} = \int_{a_m}^{b_m} (u' - u_m)^k\, K(u_1, u')\, du' \quad . \qquad (2.4\text{-}4)$$

The relation (2.4-4) is the defining relation for the moment of
degree k of the kernel centered around the mesh point u_m. The
relation (2.4-3) is a system of (2K+1) equations whose solution
determines the weighting factors in terms of the moments. A
closed form solution of the system of equations (2.4-3) is obtained
by expanding the right side of (2.4-1) and using (2.4-4):

50

$$K_{\ell mn} = \sum_{k=0}^{2K} C_{mnk} M_{\ell mk} \quad , \qquad (2.4\text{-}5)$$

where

$$C_{mnk} = \frac{1}{k! \, Q'(u_n)} \left[\frac{d^k}{dx^k} \frac{Q_m(x)}{(x-u_n)} \right]_{x=u_m} \quad . \qquad (2.4\text{-}6)$$

The relations (2.4-4), (2.4-5) and (2.4-6) show that the weighting factors are obtained by a product of a matrix C_{mn} which depends only on the mesh point distribution, and the moment matrix which depends only on the local character of the kernel in the neighborhood of the mesh point u_m.

An evaluation of the moments defined by (2.4-4) should account for the singular nature of the kernel. In Section 2.2 it has been shown that the general form of an axisymmetric kernel can be written:

$$K(u_\ell, u') = S_\ell(u') \ln w_\ell(u') + R_\ell(u') \quad , \qquad (2.4\text{-}7)$$

where from (2.2-26d), (2.2-30a), (2.2-34b) and (2.2-45a)

$$w_\ell(u') = \frac{(z_\ell - z')^2 + (\rho_\ell - \rho')^2}{(z_\ell - z')^2 + (\rho_\ell + \rho')^2} \quad . \qquad (2.4\text{-}8)$$

The singular point of the kernel occurs at $u' = u_\ell$. It is convenient to consider the functions S_ℓ and R_ℓ as being defined by two different expressions depending on the value of u'. Thus, if u' is not close to u_ℓ, S_ℓ is defined to identically zero and R_ℓ is defined by applying (2.2-47a) to (2.2-46) and using (2.2-48)

51

through (2.2-50). If u' is close to u_ℓ, the relation (2.2-45a) is used to isolate the logarithmic part, and the S_ℓ and R_ℓ are defined uniquely by this decomposition. Both representations of the S_ℓ and the R_ℓ defined by this scheme are analytic.

The degenerate case of infinite cylinders can be treated in the same manner. For this case, it can be seen from (2.2-29) and from the form of the Hankel function for small arguments that

$$w_\ell^2(u') = (k^2-\sigma^2) \, [\, (z_\ell-z')^2 + (x_\ell-x')^2] \, /2 \; . \qquad (2.4-9)$$

Using the decomposition defined by (2.4-7), the moments can be written

$$M_{\ell mk} = S_{\ell mk} + R_{\ell mk} \; , \qquad (2.4-10a)$$

where

$$S_{\ell mk} = \int_{a_m}^{b_m} (u'-u_m)^k \, S_\ell(u') \, \ln w_\ell(u') \, du' \; , \qquad (2.4-10b)$$

and

$$R_{mk} = \int_{a_m}^{b_m} (u'-u_m)^k \, R_1(u') \, du' \; . \qquad (2.4-10c)$$

The quadrature formulae which have been used for the evaluation of (2.4-10b) are based on an approximate evaluation of the integrals

$$T_k(x) = \int_o^x u^k \, F(u) \, \ln w(u) \, du \; , \qquad (2.4-11)$$

52

where $F(u)$ is an arbitrary cubic and $w(u)$ is a slowly varying function of u which vanishes only at the lower limit of the integration interval. The approximation to T_k can be written:

$$T_k(x) = x^{k+1}[T_{k1} F(0) + T_{k2} F(\beta_k x) + T_{k3} F(x)] . \quad (2.4-12)$$

The values of βk and the T_{kn}, $n = 1...3$ are determined from the fact that (2.4-12) should hold for arbitrary cubics, $F(u)$. It is straightforward to show that

$$\beta_k = \frac{W_{k+3} - W_{k+2}}{W_{k+2} - W_{k+1}} , \quad (.24-13a)$$

$$T_{k3} = \frac{W_{k+2} - \beta_k W_{k+1}}{1 - \beta_k} , \quad (2.4-13b)$$

$$T_{k2} = \frac{W_{k+1} - W_{k+2}}{\beta_k(1 - \beta_k)} , \quad (2.4-13c)$$

$$T_{k1} = W_k - T_{k2} - T_{k3} , \quad (2.4-13d)$$

where

$$W_k = \frac{1}{x^{k+1}} \int_0^x u^k \ln w(u) \, du . \quad (2.4-14)$$

The evaluation of the moments W_k will be discussed presently. First it is convenient to point out that under the same assumptions on F,

$$\int_0^x u^k F(u) \, du = x^{k+1} [\bar{T}_{k1} F(0) + \bar{T}_{k2} F(\bar{\beta}_k x) + \bar{T}_{k3} F(x)] ,$$

$$(2.4-15)$$

53

where the expressions for the barred-quantities in (2.4-15) are determined from (2.4-13) by substituting for W_k, the expressions

$$\bar{W}_k = \frac{1}{x^{k+1}} \int_o^x u^k \, du = \frac{1}{k+1} \quad . \tag{2.4-16}$$

The evaluation of the W_k defined in (2.4-14) can be performed approximately by an integration by parts to obtain

$$W_k = \frac{1}{k+1} \ln w(x) - \frac{1}{(k+1)x^{k+1}} \int_o^x \frac{u^{k+1}}{w} \frac{\partial w}{\partial u} \quad . \tag{2.4-17a}$$

Now the function $\frac{u}{w} \frac{\partial w}{\partial u}$ is an analytic function of u, and the assumption that it is slowly varying allows application of (2.4-15). Thus:

$$W_k = \frac{1}{k+1} \left[\ln w(x) - \bar{T}_{k1} \left(\frac{u}{w} \frac{\partial w}{\partial u} \right)_0 - \bar{T}_{k2} \left(\frac{u}{w} \frac{\partial w}{\partial u} \right)_{\bar{\beta}_k x} - \bar{T}_{k3} \left(\frac{u}{w} \frac{\partial w}{\partial u} \right)_x \right] . \tag{2.4-17b}$$

By breaking up the interval of integration in (2.4-10) into two parts: $a_m < u < u_m$ and $u_m < u < b_m$ and applying (2.4-11) - (2.4-17), the values of the moments are determined, subject to the assumption that the R_ℓ and the S_ℓ vary no faster than cubics over a half mesh point spacing.

54

3. ANALYSIS OF AN ELLIPTIC DOME ABOUT
A CIRCULAR TRANSDUCER

The dome-transducer model described in this section is shown in Fig. 3-1. The transducer is described by the circle $r = a$ in polar coordinates r and θ. The dome lies along the curve $\xi = \xi_0$ in elliptic coordinates ξ and η. The pressure field between the transducer and dome will be denoted by p_1 and that exterior to the dome by p_2.

At the transducer surface a fluid particle velocity distribution is specified to simulate the velocity distribution across the active array. This velocity distribution is taken to be two-dimensional, that is, the velocity v_j of the elements of the jth stave is assumed to extend indefinitely along the axial direction of the circular cylinder. The mathematical representation of this velocity distribution is

$$v_{(\theta)} = \begin{cases} |v_j| e^{-i\omega t}, & \theta_j - \alpha < \theta < \theta_j + \alpha \\ 0, & \text{elsewhere.} \end{cases} \tag{3-1}$$

Here θ_j is the angular location of the center of the jth stave and α is half the stave angular width. This distribution may be expanded in a Fourier series [7],

$$v_{(\theta)} = e^{-i\omega t} \sum_{n=0}^{\infty} \delta_n^c \cos n\theta + \delta_n^s \sin n\theta . \tag{3-2}$$

The solution p_1 of the wave equation may be represented in several ways. In order to match the boundary condition at $r = a$ it is convenient to use the Bessel function expansion, which is characteristic of circular cylindrical coordinates:
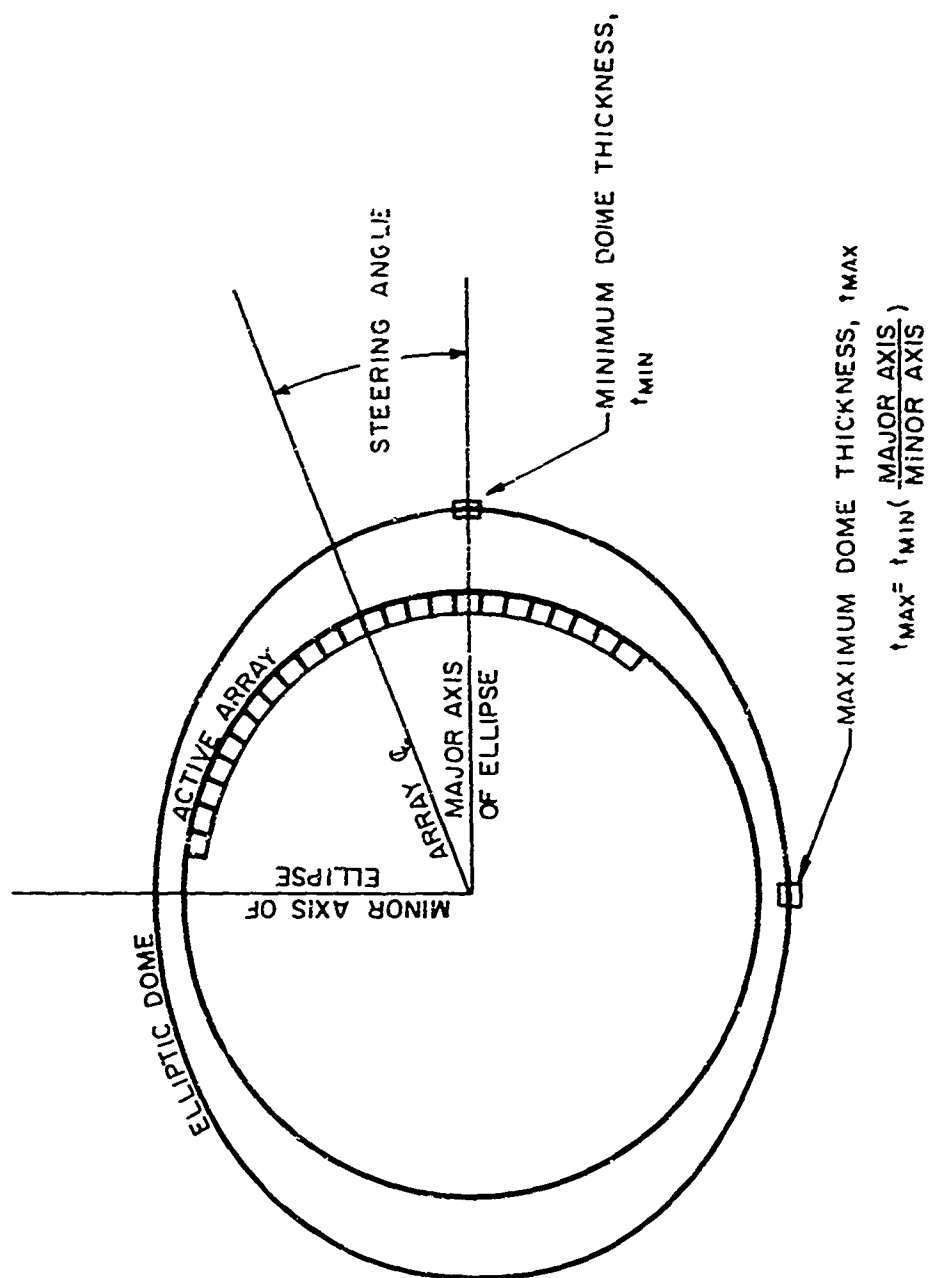
55

FIG. 3-I-GEOMETRY OF ELLIPTIC DOME AND CIRCULAR TRANSDUCER

STEERING ANGLE

MINIMUM DOME THICKNESS, t_{MIN}

MAXIMUM DOME THICKNESS, t_{MAX}

$$t_{MAX} = t_{MIN} \left(\frac{MAJOR\ AXIS}{MINOR\ AXIS} \right)$$

ELLIPTIC DOME

ACTIVE ARRAY

ARRAY &

MAJOR AXIS OF ELLIPSE

MINOR AXIS OF ELLIPSE

56

$$P_1 = \sum_{n=0}^{\infty} \left[A_n^C J_n(kr) + B_n^C N_n(kr) \right] \cos n\theta$$

$$+ \left[A_n^S J_n(kr) + B_n^S N_n(kr) \right] \sin n\theta \qquad (3\text{-}3)$$

Here J_n and N_n are, respectively, the Bessel and Neumann functions of order n and argument kr. The unknown coefficients A_n^C, A_n^S, B_n^C and B_n^S are to be determined by matching boundary conditions at the transducer and at the dome. The radial component of the fluid velocity is related to the pressure field by

$$v = \frac{1}{i\omega\rho} \frac{\partial p}{\partial r} .$$

This relation, in conjunction with Eqs. (3-2) and (3-3), implies

$$A_n^C J_n'(ka) + B_n^C N_n'(ka) = i\rho c\, \delta_n^C \qquad (3\text{-}4)$$

and

$$A_n^S J_n'(ka) + B_n^S N_n'(ka) = i\rho c\, \delta_n^S . \qquad (3\text{-}5)$$

The primes on the Bessel and Neumann functions designate differentiation with respect to argument.

According to Assumptions 7 and 8 in Section 1, a pressure difference $\Delta p(\eta)e^{-i\omega t}$ across the surface produces a normal vibrational displacement $w(\eta)e^{-i\omega t}$ which is related to the pressure difference by

57

$$\dot{p}(r) = -\omega^2 \sigma_s \, w(\eta) \ . \tag{3-6}$$

Here σ_s is the shell surface mass density.

General solutions to the wave equation may be written for the pressure fields inside and outside the shell in terms of elliptic coordinates:

$$P_1 = \sum_{n=0}^{\infty} \left[\alpha_n^e \, C e_n(\xi) + \beta_n^e \, Fey_n(\xi) \right] \, ce_n(\eta)$$

$$+ \left[\alpha_n^o \, Se_n(\xi) + \beta_n^o \, Gey_n(\xi) \right] \, se_n(\eta) \ , \tag{3-7}$$

$$P_2 = \sum_{n=0}^{\infty} \gamma_n^e \, Me_n(\xi) \, ce_n(\eta) + \gamma_n^o \, Ne_n(\xi) \, se_n(\eta) \ . \tag{3-8}$$

In the above equations, $ce_n(\eta)$ and $se_n(\eta)$ are Mathieu functions and $Ce_n(\xi)$, $Fey_n(\xi)$, $Se_n(\xi)$, and $Gey_n(\xi)$ are associated Mathieu functions. The Hankel type associated Mathieu functions in Eq. (3-8) are defined by $Me_n = Ce_n + i\, Fey_n$, $Ne_n = Se_n + i\, Fey_n$. These functions insure that there is only outgoing radiation in regions outside the dome. The α_n^e, α_n^o, β_n^e, β_n^o, γ_n^e and γ_n^o are unknown coefficients which are to be determined by matching boundary conditions at the dome and transducer.

At the inner and outer surfaces of the dome the fluid velocity component normal to the dome is equal to $\frac{\partial w}{\partial t}$. Matching these boundary conditions at the dome middle surface, $\xi = \xi_o$, gives

$$\frac{1}{i\omega\rho} \left(\frac{\partial P_1}{\partial n} \right)_{\xi = \xi_o} = \frac{\partial w}{\partial t} = \frac{1}{i\omega\rho} \left(\frac{\partial P_2}{\partial n} \right)_{\xi = \xi_o} \tag{3-9}$$

58

In elliptic coordinates the normal derivative is computed according to

$$\left(\frac{\partial p}{\partial n}\right)_{\xi=\xi_o} = \frac{1}{h\sqrt{\sinh^2\xi_o + \sin^2\eta}} \left(\frac{\partial p}{\partial \xi}\right)_{\xi=\xi_o} , \tag{3-10}$$

where h is half the interfocal separation. Combining Eqs. (3-6), (3-9), and (3-10) yields

$$[p_1 - p_2]_{\xi=\xi_o} = -\frac{\sigma_s}{\rho h\sqrt{\sinh^2\xi_o + \sin^2\eta}} \left(\frac{\partial p_2}{\partial \xi}\right)_{\xi=\xi_o} , \tag{3-11}$$

or

$$\sum_{n=0}^{\infty} \left\{ \left[\alpha_n^e Ce_n(\xi_e) + \beta_n^e Fey_n(\xi_o) - \gamma_n^e Me_n(\xi_o)\right] ce_n(\eta) \right.$$

$$+ \left[\alpha_n^o Se_n(\xi_o) + \beta_n^o Gey_n(\xi_o) - \gamma_n^o Ne_n(\xi_o)\right] se_n(\eta) \right\}$$

$$= \frac{\sigma_s}{\rho h\sqrt{\sinh^2\xi_o + \sin^2\eta}} \sum_{n=0}^{\infty} \gamma_n^e Me_n'(\xi_o) se_n(\eta) + \gamma_n^o Ne_n'(\xi_o) se_n(\eta) . \tag{3-12}$$

where the primes on the Me_n and Ne_n designate differentiation with respect to argument. There will be coupling among the $ce_n(\eta)$ and $se_n(\eta)$ modes unless σ_s is made to vary as $\sqrt{\sinh^2\xi_o + \sin^2\eta}$. This variation in σ_s can be considered as resulting from a dome thickness which varies as the distance between confocal ellipses. Assuming such a variation of σ_s and employing the linear independence of the Mathieu functions leads to the relations

$$\alpha_n^e \, Ce_n(\xi_o) + \beta_n^e \, Fey_n(\xi_o) - \gamma_n^e \, Me_n(\xi_o) = -\frac{\sigma}{\rho h} \, \gamma_n^e \, Me_n'(\xi_o) \quad , \quad (3\text{-}13)$$

$$\alpha_n^o \, Se_n(\xi_o) + \beta_n^o \, Gey_n(\xi_o) - \gamma_n^o \, Ne_n(\xi_o) = -\frac{\sigma}{\rho h} \, \gamma_n^o \, Ne_n'(\xi_o) \quad , \quad (3\text{-}14)$$

where $\sigma_s = \sigma \sqrt{\sinh^2 \xi_o + \sin^2 \eta}$. The condition in Eq. (3-9) may be simplified by using Eqs. (3-7) and (3-8) and the linear independence of the Mathieu functions. Thus,

$$\alpha_n^e \, Ce_n'(\xi_o) + \beta_n^e \, Fey_n'(\xi_o) = \gamma_n^e \, Me_n'(\xi_o) \quad , \quad\quad (3\text{-}15)$$

$$\alpha_n^o \, Se_n'(\xi_o) + \beta_n^o \, Gey_n'(\xi_o) = \gamma_n^o \, Ne_n'(\xi_o) \quad . \quad\quad (3\text{-}16)$$

Equations (3-13)-(3-15) may be used to express α_n^e, α_n^o, β_n^e, and β_n^o in terms of γ_n^e and γ_n^o . These results are

$$\alpha_n^e = \left[1 - \frac{R}{W} \, Me_n'(\xi_o) \, Fey_n'(\xi_o)\right] \gamma_n^e \quad , \quad\quad (3\text{-}17)$$

$$\beta_n^e = \left[i + \frac{R}{W} \, Me_n'(\xi_o) \, Ce_n'(\xi_o)\right] \gamma_n^e \quad , \quad\quad (3\text{-}18)$$

$$\alpha_n^o = \left[1 - \frac{R}{W} \, Ne_n'(\xi_o) \, Gey_n'(\xi_o)\right] \gamma_r^o \quad , \quad\quad (3\text{-}19)$$

$$\beta_n^o = \left[i + \frac{R}{W} \, Ne_n'(\xi_o) \, Se_n'(\xi_o)\right] \gamma_n^o \quad . \quad\quad (3\text{-}20)$$

Here W is the Wronskian of the associated Mathieu functions and $R = \frac{\sigma}{\rho h}$. For the definition of these functions used in the final computations, $W = 2/\pi$.

At this point, the pressure field p_1 inside the dome has been represented in both circular and elliptic coordinates.

The two representations must be identically equal at all points within the dome. A set of equations for determining the unknown coefficients γ_n^e and γ_n^o can be found by demanding that the two representations of p_1 be equal. This procedure is facilitated by employing the expansions of the elliptic coordinate eigenfunctions in terms of the circular coordinate eigenfunctions. These are:

$$Ce_n(\xi) \, ce_n(\eta) = \sum_{m=0}^{\infty} (-1)^{m+q} A_p^n J_p(kr) \cos p \, \theta \begin{cases} p = 2m, \text{ n even} \\ p = 2m+1, \text{ n odd} \\ q = n/2, \text{ n even} \\ q = \frac{n-1}{2}, \text{ n odd} \end{cases} \quad (3\text{-}21)$$

$$Fey_n(\xi) \, ce_n(\eta) = \sum_{m=0}^{\infty} (-1)^{m+q} A_p^n N_p(kr) \cos p \, \theta \, , \qquad (3\text{-}22)$$

$$Se_n(\xi) \, se_n(\eta) = \sum_{m=0}^{\infty} (-1)^{m+q} B_p^n J_p(kr) \sin p \, \theta \, , \qquad (3\text{-}23)$$

$$Gey_n(\xi) \, se_n(\eta) = \sum_{m=0}^{\infty} (-1)^{m+q} B_p^n N_p(kr) \sin p \, \theta \, . \qquad (3\text{-}24)$$

The A_p^n and B_p^n are the Fourier coefficients in the expansions

$$ce_n(\eta) = \sum_{m=0}^{\infty} A_p^n \cos p \, \eta \, ,$$

$$se_n(\eta) = \sum_{m=0}^{\infty} B_p^n \sin p \, \eta \, .$$

61

By equating the expressions in Eqs. (3-3) and (3-7) and substituting Eqs. (3-21)-(3-24) for the elliptic coordinate eigenfunctions, the coefficients A_n^C, B_n^C, A_n^S, and B_n^S are found in terms of α_n^e, β_n^e, α_n^o, and β_n^o. Then Eqs. (3-4), (3-5), (3-17), (3-18), (3-19), and (3-20) may be used to eliminate all the coefficients except the γ_n^e and γ_n^o. The final equations are shown in Table 3-I.

The equations in Table 3-I constitute four infinite sets of linear equations in the γ_n^e and γ_n^o. Numerical experimentation indicates that they are convergent in the following sense. Suppose a set of 2M of the γ_n^e and 2M of the γ_n^o are obtained by solving the first M equations of each set, truncating the sum in each equation after the Mth term. If the first N of the γ_{2n}^e, γ_{2n+1}^e, γ_{2n+1}^o, and γ_{2n+2}^o do not change in, say, the first six significant figures as M is increased past some value, denoted by M_N, then the equations are said to have converged to N terms for an M_N by M_N set of equations. When a sufficient number of γ_n^e and γ_n^o have been computed in the above manner for the series in Eq. (3-8) to converge, the problem solution is completed.

62

TABLE 3-I

EQUATIONS FOR γ_n^e and γ_n^o

$$\sum_{n=0}^{\infty} (-1)^n A_{2n} \left\{ H'_{2m}(ka) - \frac{R}{W} Me'_{2n}(\xi_o) \right\} J'_{2m}(ka) Fey'_{2n}(\xi_o) - N'_{2m}(ka) Ce'_{2n}(\xi_o) \gamma^e_{2n} = i\rho c (-1)^m \delta^c_{2m}$$

$$\sum_{n=0}^{\infty} (-1)^n A_{2n+1} \left\{ H'_{2m+1}(ka) - \frac{R}{W} Me'_{2n+1}(\xi_o) \right\} J'_{2m+1}(ka) Fey'_{2n+1}(\xi_o) - N'_{2m+1}(ka) Ce'_{2n+1}(\xi_o) \gamma^e_{2n+1} = i\rho c (-1)^m \delta^e_{2m+1}$$

$$\sum_{n=0}^{\infty} (-1)^n B_{2n+1} \left\{ H'_{2m+1}(ka) - \frac{R}{W} Ne'_{2n}(\xi_o) \right\} J'_{2m+1}(ka) Gey'_{2n+1}(\xi_o) - N'_{2m+1}(ka) Se'_{2n+1}(\xi_o) \gamma^o_{2n+1} = i\rho c (-1)^m \delta^s_{2m+1}$$

$$\sum_{n=0}^{\infty} (-1)^n B_{2n+2} \left\{ H'_{2m+2}(ka) - \frac{R}{W} Ne'_{2n+2}(\xi_o) \right\} J'_{2m+2}(ka) Gey'_{2n+2}(\xi_o) - N'_{2m+2}(ka) Se'_{2n+2}(\xi_o) \gamma^o_{2n+2} = i\rho c (-1)^m \delta^s_{2m+2}$$

63

4. THREE-DIMENSIONAL CYLINDER-DOME MODEL

The mathematical model described in this section (Fig. 4-1) is an extension of the two-dimensional cylindrical transducer and concentric shell model. In the present model the active region of the transducer is finite in height. This generalization of the model permits the computation of three-dimensional beam patterns and directivity indices of cylindrical arrays.

The pressure field of a single rectangular element will first be obtained. Then superposition will be employed to determine the array beam pattern. Let the particular element chosen be such that the x-z plane passes through its center. The time dependent factor ($e^{-i\omega t}$) will be suppressed in the following.

The velocity distribution on the cylinder, r=a, is non-vanishing only on the element surface. That is,

$$v = \begin{cases} v_o & |z - z_c| < z_o, \quad |\varpi| < \varpi_o \\ 0 & \text{elsewhere} \end{cases} , \qquad (4\text{-}1)$$

where z_c is the z coordinate of the element center, z_o is the half height of the element, and ϖ_o is the half angular width of the element. It is convenient to take the Fourier transform of all the fields which depend on the z coordinate.

The Fourier transform of v is defined to be

$$\bar{v} = \begin{cases} \dfrac{1}{\sqrt{2\pi}} \displaystyle\int_{-\infty}^{\infty} v \, e^{-i\lambda z} \, dz & |\varpi| < \varpi_o \\ 0 & |\varphi| > \varphi_o \end{cases} . \qquad (4\text{-}2)$$
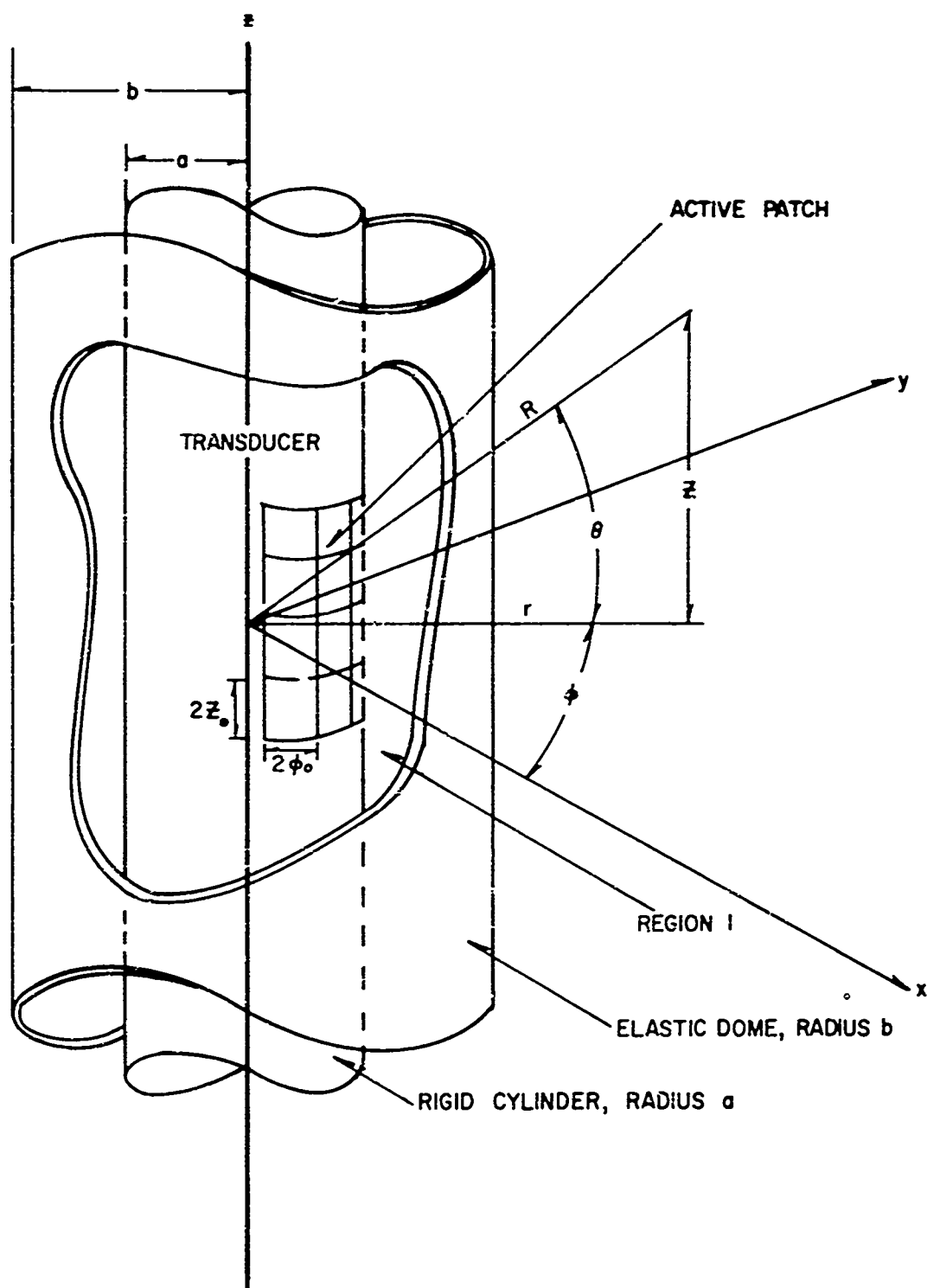
FIG. 4-I - GEOMETRY FOR A THREE DIMENSION CYLINDRICAL
TRANSDUCER RADIATING INSIDE A CONCENTRIC DOME

Substituting Eq. (4-1) into Eq. (4-2) yields

$$\bar{v} = \left\{ \begin{array}{ll} \dfrac{\sqrt{2}\, v_o z_o\, e^{-i\lambda z_c}}{\sqrt{\ }} \left(\dfrac{\sin \lambda z_o}{\lambda z_o} \right) & |\omega| < \omega_o \\[3ex] o & |\omega| > \omega_o \end{array} \right\} . \qquad (4\text{-}3)$$

In like manner, the transform of the pressure field p is defined to be

$$\bar{p} = \frac{1}{\sqrt{2\ }} \int_{-\infty}^{\infty} p e^{-i\lambda z}\, dz . \qquad (4\text{-}4)$$

The pressure field satisfies the Helmholtz equation,

$$\nabla^2 p + k^2 p = 0 . \qquad (4\text{-}5)$$

Taking the Fourier transform of Eq. (4-5) gives

$$\nabla^2 \bar{p} + K^2 \bar{p} = 0 , \qquad (4\text{-}6)$$

where $K^2 = k^2 - \lambda^2$.

The boundary condition at the transducer-fluid interface is

$$i\omega\rho v \Big]_{r=a} = \frac{\partial p}{\partial r}\Big]_{r=a} \qquad (4\text{-}7)$$

The Fourier transform of Eq. (4-7) is

$$i\omega\rho \bar{v} \Big]_{r=a} = \frac{\partial \bar{p}}{\partial r}\Big]_{r=a} . \qquad (4\text{-}8)$$

The Flügge shell equations are assumed to describe the behavior of the dome [8]. The following dynamic equations are Flügge's equations with an added D'Alembert force. The fluid is inviscid and therefore there are no external forces acting in the φ or z directions:

$$b^2 \frac{\partial^2 u_z}{\partial z^2} + \frac{1-\nu}{2} \frac{\partial^2 u_z}{\partial \varphi^2} + b\frac{(1+\nu)}{2} \frac{\partial^2 u_\varphi}{\partial z \partial \varphi} + b\nu \frac{\partial u_r}{\partial z} + k^* \left[\frac{1-\nu}{2} \frac{\partial^2 u_z}{\partial \varphi^2} - b^3 \frac{\partial^3 u_r}{\partial z^3}\right.$$

$$\left. + b\frac{(1-\nu)}{2} \frac{\partial^3 u_r}{\partial z \partial \varphi^2}\right] + \frac{b^2}{D} \rho_s h \frac{\partial^2 u_z}{\partial t^2} = 0 \quad , \tag{4-9}$$

$$b \left(\frac{1+\nu}{2}\right)\frac{\partial^2 u_z}{\partial z \partial \varphi} + \frac{\partial^2 u_\varphi}{\partial \varphi^2} + b^2 \left(\frac{1-\nu}{2}\right) \frac{\partial^2 u_\varphi}{\partial z^2} + \frac{\partial u_r}{\partial \varphi} + k^* \left[\frac{3}{2} b^2(1-\nu) \frac{\partial^2 u_\varphi}{\partial z^2}\right.$$

$$\left. - b^2 \left(\frac{3-\nu}{2}\right) \frac{\partial^3 u_r}{\partial z^2 \partial \varphi}\right] + \frac{b^2}{D} \rho_s h \frac{\partial^2 u_\varphi}{\partial t^2} = 0 \quad , \tag{4-10}$$

$$b\nu \frac{\partial u_z}{\partial z} + \frac{\partial u_\varphi}{\partial \varphi} + u_r + k^* \left[b\left(\frac{1-\nu}{2}\right) \frac{\partial^3 u_z}{\partial z \partial \varphi^2} - b^3 \frac{\partial^3 u_z}{\partial z^3} - b^2\left(\frac{3-\nu}{2}\right) \frac{\partial^3 u_\varphi}{\partial z^2 \partial \varphi}\right.$$

$$\left. + b^4 \frac{\partial^4 u_r}{\partial z^4} + 2b^2 \frac{\partial^4 u_r}{\partial z^2 \partial \varphi^2} + \frac{\partial^4 u_r}{\partial \varphi^4} + 2\frac{\partial^2 u_r}{\partial \varphi^2} + u_r\right] - \frac{b^2}{D}\left[p_1 - p_2 + \rho_s h \frac{\partial^2 u_r}{\partial t^2}\right] = 0.$$

$$\tag{4-11}$$

The quantities in Eqs. (4-9) - (4-11) are: b, the middle radius of the dome; ν, Poisson's ratio; ρ_s, the density of the dome material; h, the thickness of the dome; $k^* = \frac{h^2}{12b^2}$; $D = E_s h$; and u_z, u_φ,

and u_r, the displacement components of the middle surface of the dome in the z, φ, and r directions, respectively.

Equations (4-9) - (4-11) must be Fourier-transformed. It is assumed that the displacements may be expressed as Fourier series.

$$u_z = \sum_{n=0}^{\infty} U_n(z) \cos n\varphi \ , \tag{4-12}$$

$$u_\varphi = \sum_{n=0}^{\infty} V_n(z) \sin n\varphi \ , \tag{4-13}$$

$$u_r = \sum_{n=0}^{\infty} W_n(z) \cos n\varphi \ . \tag{4-14}$$

The Fourier transforms of u_z, u_φ, and u_r are defined respectively as

$$\bar{u}_z = \frac{1}{\sqrt{2\pi}} \int_{-\infty}^{\infty} u_z \, e^{-i\lambda z} \, dz \ , \tag{4-15}$$

$$\bar{u}_\varphi = \frac{1}{\sqrt{2\pi}} \int_{-\infty}^{\infty} u_\varphi \, e^{-i\lambda z} \, dz \ , \tag{4-16}$$

$$\bar{u}_r = \frac{1}{\sqrt{2\pi}} \int_{-\infty}^{\infty} u_r \, e^{-i\lambda z} \, dz \ . \tag{4-17}$$

The displacement components of the dome, Eqs. (4-12) - (4-14), can now be Fourier-transformed:

$$\bar{u}_z = \sum_{n=0}^{\infty} \bar{U}_n (\lambda) \cos n\varphi , \qquad (4\text{-}18)$$

$$\bar{u}_\varphi = \sum_{n=0}^{\infty} \bar{V}_n (\lambda) \sin n\varphi , \qquad (4\text{-}19)$$

$$\bar{u}_r = \sum_{n=0}^{\infty} \bar{W}_n (\lambda) \cos n\varphi . \qquad (4\text{-}20)$$

It is now convenient to Fourier-transform Flügge's shell equations. In addition to Fourier-transforming Eqs. (4-9) - (4-11), the transformed Fourier series representation for the displacements, Eqs. (4-18) - (4-20), are substituted into Flügge's equations. To reiterate Assumption 4, the displacement components have harmonic time dependence. The relationships between transformed displacement components and transformed velocity components of the shell are therefore:

$$\tilde{v}_z = -i\omega \, \bar{u}_r ,$$

$$\tilde{v}_\varphi = -i\omega \, \bar{u}_\varphi ,$$

$$\tilde{v}_r = -i\omega \, \bar{u}_r ,$$

where $\bar{v}_z$, $\bar{v}_\varphi$, and $\bar{v}_r$ are respectively the transformed velocity components in the z, φ, and r coordinate directions. The transformed shell equations, in terms of velocity components, can be written as follows:

69

$$\bar{U}_n \left[-\lambda^2 b^2 - n^2 \left(\frac{1-\nu}{2}\right)(1+k^*) + \frac{\lambda^2 b^2 \rho_s h}{D} \right] + \bar{V}_n \left[i\lambda bn \frac{(1+\nu)}{2} \right] +$$

$$\bar{W}_n \left[i\lambda b\nu + k^* \left(ib^3\lambda^3 - i\lambda bn^2 \frac{(1-\nu)}{2} \right) \right] = 0 , \qquad (4\text{-}21)$$

$$\bar{U}_n \left[-i\lambda bn \frac{(1+\nu)}{2} \right] + \bar{V}_n \left[-n^2 - \lambda^2 b^2 \frac{(1-\nu)}{2} - k^*\lambda^2 \frac{3}{2} b^2 (1-\nu) + \frac{b^2 \lambda^2 \rho_s h}{D} \right] +$$

$$\bar{W}_n \left[-n - k^*\lambda^2 b^2 n \frac{(3-\nu)}{2} \right] = 0 , \qquad (4\text{-}22)$$

$$A_n \left[-\frac{b^2}{D} J_n(Kb) \right] + B_n \left[-\frac{b^2}{D} N_n(Kb) \right] + C_n \left[\frac{b^2}{D} H_n(Kb) \right] +$$

$$\bar{U}_n \left[i\lambda b\nu - k^* i\lambda bn^2 \frac{(1-\nu)}{2} + k^* i\lambda^3 b^3 \right] +$$

$$\bar{V}_n \left[n + k^*\lambda^2 b^2 n \left(\frac{3-\nu}{2}\right) \right] + \bar{W}_n \left[1 + k^* (\lambda^4 b^4 + 2\lambda^2 b^2 n^2 + n^4) - \right.$$

$$\left. k^* (2n^2 - 1) - \frac{b^2}{D} \rho_s h\omega^2 \right] = 0 . \qquad (4\text{-}23)$$

To obtain Eq. (4-23) from Eq. (4-11), it was necessary to assume solution forms for the pressures p_1 and p_2. The pressure in region 1 (see Fig. 4-1) is denoted by p_1 and in region 2 by p_2. When Eq. (4-11) is Fourier-transformed, the pressures p_1 and p_2 transform into $\bar{p}_1$ and $\bar{p}_2$, respectively. The transformed pressures $\bar{p}_1$ and $\bar{p}_2$ must satisfy the transformed Helmholtz equation, Eq. (4-6). The form of the solution to Eq. (4-6) is known and can be written as

$$\bar{p}_1 = \sum_{n=0}^{\infty} [A_n J_n(Kr) + B_n N_n(Kr)] \cos n\varphi , \qquad (4\text{-}24)$$

$$\bar{p}_2 = \sum_{n=0}^{\infty} C_n H_n(Kr) \cos n\varphi . \qquad (4\text{-}25)$$

It is necessary to require that $K \neq 0$ to insure that the Bessel function of the second kind in Eq. (4-24) remains finite in the range of interest.

One boundary condition which must be satisfied is the transducer-fluid interface condition at r=a, Eq. (4-8). The pressure is given by $\bar{p}_1$, and $\bar{v}$ is given by Eq. (4-3). The transformed boundary condition at r=a yields the relation,

$$A_n J_n'(Ka) + B_n N_n'(Ka) = \frac{i\omega\rho \sqrt{2} \, \varepsilon_n v_o z_o \varphi_o}{K(\pi)^{3/2}} \frac{\sin \lambda z_o}{\lambda z_o} \frac{\sin n\varphi_o}{n\varphi_o} , \qquad (4\text{-}26)$$

where the prime denotes the differentiation with respect to argument, and ε_n is the Neumann symbol $\varepsilon_o = 1$, $\varepsilon_n = 2 \, n > o$. Two more boundary conditions must be satisfied at the middle surface of the shell. The radial velocity of the middle surface of the shell must equal the normal gradient of the pressure evaluated at r=b. This requirement applies to representations of the pressure both inside and outside the shell.

Satisfaction of the two shell middle surface boundary conditions requires that

$$A_n J_n'(Kb) + B_n N_n'(Kb) = \frac{\omega^2 \rho \, \bar{W}_n}{K} , \qquad (4\text{-}27)$$

$$K C_n H_n^{(1)'}(Kb) = \omega^2 \rho \, \bar{W}_n . \qquad (4\text{-}28)$$

71

The solution is now such that there are six equations and six unknowns. Equations (4-21) - (4-23), (4-26), and (4-27) - (4-28) are the six equations, and A_n, B_n, C_n, $\overline{U}_n$, $\overline{V}_n$, and $\overline{W}_n$ are the unknowns. After tedious algebra, the unknown coefficients C_n may be obtained:

$$C_n(\lambda) = \frac{\Gamma_n}{H_n^{(1)\prime}(Ka) + \dfrac{hE_s \pi K^2 H_n^{(1)\prime}(Kb)\Delta_n}{2b\omega^2_0}\left\{m_9 + \dfrac{2m_2 m_6 m_3 - m_3^2 m_5 + m_1 m_6^2}{(m_1 m_5 + m_2)^2}\right\}}$$

$$(4-29)$$

where

$$\Gamma_n = \frac{i\omega\rho\sqrt{2}\,\varepsilon_n v_0 z_0 \omega_0}{K\,(\pi)^{3/2}}\,\frac{\sin \lambda z_0}{\lambda z_0}\,\frac{\sin n\,\varphi_0}{n\,\varphi_0}\;,$$

$$\Delta_n = J_n'(Ka)\,N_n'(Kb) - J_n'(Kb)\,N_n'(Ka)\;,$$

$$m_1 = -\lambda^2 b^2 - n^2\left(\frac{1-\nu}{2}\right)(1 + k^*) + \frac{\omega^2 \rho_s b^2 h}{D}\;,$$

$$m_2 = i\lambda bn\left(\frac{1+\nu}{2}\right)\;,$$

$$m_3 = i\lambda b\nu + k^*\left[i\lambda^3 b^3 - i\lambda bn^2\left(\frac{1-\nu}{2}\right)\right]\;,$$

$$m_5 = -n^2 - \lambda^2 b^2\left(\frac{1-\nu}{2}\right) - k^*\lambda^2\,\frac{3}{2}\,b^2(1-\nu) + \frac{b^2\omega^2\rho_s h}{D}\;,$$

$$m_6 = -n - k^* \lambda^2 b^2 n \left(\frac{3-\nu}{2} \right) ,$$

$$m_9 = 1 + k^* (\lambda^2 b^2 + n^2)^2 - k^* (2n^2 - 1) - \frac{b^2 \rho_s h \omega^2}{D}.$$

With the coefficient C_n thus obtained, the transformed pressure in region 2 is determined. The problem to this stage has been even about the x-z plane. If $\omega \neq 0$ as assumed, but if instead the element is located at ω_c then $\omega \rightarrow (\omega - \omega_c)$:

$$\cos n\varphi \rightarrow \cos n(\varphi - \varphi_c)$$

$$\cos n(\varphi - \varphi_c) = \cos n\varphi_c \cos n\varphi + \sin n\varphi_c \sin n\varphi .$$

Equation (4-25) can be rewritten as,

$$\bar{p}_2 = \sum_{n=o}^{\infty} [C_n H_n^{(1)}(Kr) \cos n\varphi_c \cos n\varphi + C_n H_n^{(2)}(Kr) \sin n\varphi_c \sin n\varphi]. \qquad (4\text{-}30)$$

The inverse Fourier transform of $\bar{p}_2$ yields a formal solution for p:

$$p = \frac{1}{\sqrt{2\pi}} \int_{-\infty}^{\infty} \sum_{n=o}^{\infty} C_n(\lambda) [\cos n\varphi_c \cos n\varphi + \sin n\varphi_c \sin n\varphi] e^{i\lambda z} H_n^{(1)}(Kr) \, d\lambda. \qquad (4\text{-}31)$$

The pressure p, as written, is in terms of cylindrical polar coordinates. It will be convenient to express p in spherical coordinates (R,θ,ω). From Fig. (4-1), $r = R \cos\theta$ and $z = R \sin\theta$.

$$p = \frac{1}{\sqrt{2\pi}} \int_{-\infty}^{\infty} \sum_{n=0}^{\infty} C_n(\lambda) [\cos n\varphi_c \cos n\varphi + \sin n\varphi_c \sin n\varphi] e^{i\lambda R \sin\theta} H_n^{(1)}(KR\cos\theta) \, d\lambda. \qquad (4\text{-}32)$$

73

The crux of the problem is the evaluation of the integral in Eq. (4-32). The method of steepest descent can be applied to Eq. (4-32) [9]. The method of steepest descent is a technique to find an asymptotic approximation to a certain class of integrals, namely, integrals of the form

$$I(r) = \int_C g(z) \, e^{rf(z)} dz \quad ,$$

where r is large and positive. By applying steepest descent, it has been tacitly assumed that only farfield pressure results will be forthcoming. Equation (4-32) must be of such a form that the contour of integration can be deformed so that an asymptotic expansion of the Hankel function can be made. Further, the contour must be deformed to pass through the saddle points of $f(z)$. Equation (4-32) meets all necessary requirements for a steepest descents analysis. The results are,

$$p(R, \vartheta, \varphi) = 2\frac{e^{ikR}}{R} \sum_{n=0}^{\infty} e^{-i\frac{\pi}{2}(n+1)} G_n(\varphi, \lambda_o) \quad , \tag{4-33}$$

where

$$G_n(\varphi, \lambda_o) = \frac{1}{\sqrt{2\pi}} C_n(\lambda_o)[\cos n\varphi_c \cos n\varphi + \sin n\varphi_c \sin n\varphi] \quad , \text{ and}$$

$$\lambda_o = k \sin \varphi \quad .$$

The farfield pressure is now completely determined.

74

5. SPHERICAL TRANSDUCER-DOME MODEL

The analysis of the spherical transducer and concentric spherical dome was presented in a previous technical memorandum [10]. The earlier analysis will be outlined in this section, then the extension of the analysis necessary to compute mutual acoustic impedances will be presented.

The geometry of the spherical transducer and spherical dome is shown in Fig. 5-1. The first step in the analysis is the solution for the sound pressure radiated by a single piston. The vibrating piston will produce a sound pressure field between the dome and transducer. This pressure field is a solution to the wave equation and can be represented by the expansion,

$$P_1 = \sum_{m=0}^{\infty} \left[A_m j_m(kr) + B_m n_m(kr) \right] P_m(\cos \psi) . \quad (5\text{-}1)$$

This form is standard for solutions of the wave equation in spherical coordinates (r, ψ) if there is symmetry about the axis from which the angle ψ is measured. The P_m are Legendre polynomials of argument $\cos \psi$ and the j_m and n_m are, respectively, the spherical Bessel and Neumann functions of argument kr. The A_m and B_m are constants which can be adjusted to make the solution form fit whatever boundary conditions are prescribed on the transducer and shell surfaces. The boundary conditions arise in equating the fluid and solid velocity components normal to the fluid-solid interfaces. Velocity components tangential to the interfaces are not necessarily equal since the fluid is inviscid.

For the case at hand, the fluid velocity is equal to the piston velocity on the piston surface and is zero on the remaining transducer surface. The piston velocity, $v_0 e^{-i\omega t}$, will be considered to be purely radial, so the boundary condition at the transducer surface $r = a$ is

75
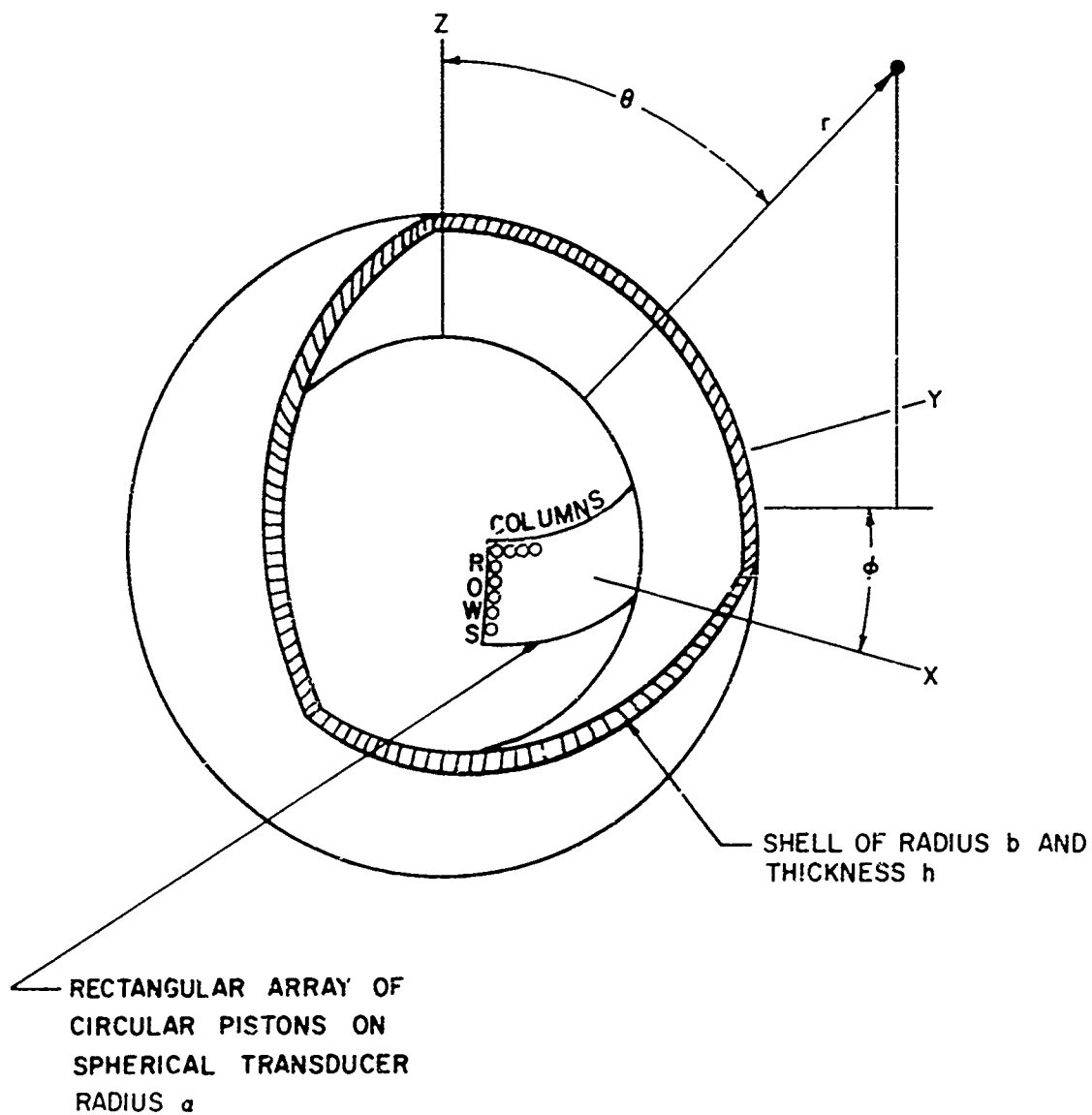
FIG. 5-I — ARRAY ON **SPHERICAL** TRANSDUCER WITHIN
CONCENTRIC SPHERICAL SHELL

76

$$\frac{k}{i\rho} \sum_{m=0}^{\infty} \left[A_m j_m'(ka) + B_m n_m'(ka) \right] P_m(\cos \tau) = \begin{cases} v_o, & 0 \le \tau < \alpha \\ 0, & \alpha < \tau \le \pi \, . \end{cases} \tag{5-2}$$

Here the angular extent of the piston is $0 \le \tau < \alpha$, the radial fluid velocity component being zero outside of this range. The primes on the j_m and n_m denote differentiation with respect to argument.

While the pressure field between the transducer and dome has the form given in Eq. (5-2), the sound pressure field p_2 outside the dome must have a form which describes only outgoing radiation for large r. This form is

$$P_2 = \sum_{m=0}^{\infty} C_m h_m(kr) P_m(\cos \tau) \, , \tag{5-3}$$

where $h_m = j_m + i n_m$ is a spherical Hankel function and the C_m are determined by the boundary condition at the outer dome surface. Since the dome is thin relative to an acoustic wavelength, it is sufficient to apply the velocity continuity condition at the dome midsurface, $r = b$, rather than at the actual fluid-dome interfaces. Thus,

$$\frac{1}{i\omega\rho} \frac{\partial P_1}{\partial r} \bigg|_{r=b} = \frac{1}{i\omega\rho} \frac{\partial P_2}{\partial r} \bigg|_{r=b} = w \, , \tag{5-4}$$

w being the radial velocity distribution of the dome. The Legendre polynomials form a complete set over the range $0 < \tau < \pi$, hence the dome velocity admits of an expansion

77

$$w = \sum_{m=0}^{\infty} W_m P_m(\cos \psi) \; . \tag{5-5}$$

Equations (5-2) and (5-5) give three conditions on the four sets of unknowns, A_m, B_m, C_m and W_m. The fourth condition must come from an analysis of the motion of the dome.

In the earlier report [10], it is shown that the application of a load distribution of the form $\alpha_m P_m(\cos \psi) e^{-i\omega t}$ to the dome will cause a velocity distribution $w = \dfrac{\alpha_m}{Z_m} P_m(\cos \psi) e^{-i\omega t}$, where Z_m is the modal impedance of the dome. The driving force on the dome in the problem under consideration is just

$$P_1 - P_2 = \sum_{m=0}^{\infty} \left[A_m j_m(kb) + B_m n_m(kb) - C_m h_m(kb) \right] P_m(\cos \psi) \; . \tag{5-6}$$

Thus the dome response is

$$w = \sum_{m=0}^{\infty} \frac{1}{Z_m} \left[A_m j_m(kb) + B_m n_m(kb) - C_m h_m(kb) \right] P_m(\cos \psi) \; . \tag{5-7}$$

Equation (5-7) is the fourth condition required to solve for the A_m, B_m, C_m, and W_m.

The solution for the expansion coefficients is straight-forward, involving only the use of the orthogonality of the Legendre functions to derive simple algebraic equations from which the expansion coefficients can be obtained. For farfield radiation characteristics, only the coefficient C_m is required. It is given by

$$C_m = v_o \frac{i\rho c}{2} \frac{P_{m-1}(\cos \alpha) - P_{m+1}(\cos \alpha)}{h'_m(ka) + \frac{Z_m}{i\rho c}(kb)^2 h'_m(kb) [j'_m(ka) \, n_m(kb)' - j'_m(kb) \, n'_m(ka)]} .$$

(5-8)

To compute the farfield distribution, the asymptotic form of $h_m(kr)$ for large r,

$$\lim_{kr \to \infty} h_m(kr) = \frac{i^{-m-1}}{kr} e^{ikr} ,$$

can be substituted into Eq. (5-3). Thus,

$$\lim_{r \to \infty} p(r,\theta) = \rho c v_o \frac{e^{i(kr-\omega t)}}{r} F(\cos \theta) ,$$

(5-9)

where

$$F(\cos \theta) = \frac{1}{2k} \sum_{m=0}^{\infty} \frac{i^{-m'} P_{m-1}(\cos \alpha) - P_{m+1}(\cos \alpha)}{h'_m(ka) + \frac{Z_m}{i\rho c}(kb)^2 h'_m(kb) [j'_m(ka) n'_m(kb) - j'_m(kb) n'_m(ka)]} .$$

This expression determines the farfield characteristics for a single piston.

The farfield sound pressure, $p(r,\theta,\phi)$, of an array of pistons can be found by superposition of the fields produced by the individual pistons. The piston whose center is at θ_J, ϕ_J on the transducer has velocity $v_J e^{-i\omega t}$. The cosine of the angle between θ, ϕ and θ_J, ϕ_J is just

79

$$\cos \psi_J = \cos \theta \cos \theta_J + \sin \theta \sin \theta_J \cos (\phi - \phi_J) \quad . \quad (5\text{-}10)$$

Superposition of the pressure fields of an array of N pistons gives

$$p(r,\theta,\phi) = \rho c \, \frac{e^{i(kr - \omega t)}}{r} \, D(\theta,\phi) \quad , \qquad (5\text{-}11)$$

where

$$D(\theta,\phi) = \sum_{J=1}^{N} v_J \, F(\cos \psi_J) \quad .$$

The farfield intensity distribution I is $\frac{1}{2\rho c} \, p^* \, p$, where the asterisk denotes the complex conjugate. Therefore,

$$I = \frac{\rho c}{2} \, \frac{1}{r^2} \, |D(\theta,\phi)|^2 \quad . \qquad (5\text{-}12)$$

The pressure field p_1 for a single piston, evaluated at the transducer surface, is found to be

$$p_1 = V_0 \, \frac{i \rho c}{2} \sum_n \Gamma_n \, [P_{n-1}(\cos \alpha) - P_{n+1}(\cos \alpha)] \, P_n(\cos \psi) \quad ,$$
$$(5\text{-}13)$$

where

$$\Gamma_n = \frac{h_n(ka) + \dfrac{Z_n}{i\rho c}(kb)^2 h_n(kb)[\, j_n(ka)n_n'(kb) - j_n'(kb)n_n(ka)]}{h_n'(ka) + \dfrac{Z_n}{i\rho c}(kb)^2 h_n'(kb)[\, j_n'(ka)n_n'(kb) - j_n'(kb)n_n'(ka)]} \quad .$$

This pressure field causes a net force on the other elements in an array.

80

By use of the addition theorem for Legendre polynomials this solution may be represented in a different polar coordinate system, whose z-axis passes through the center of a second piston. Then the total force on the second piston due to the pressure field of the first may be determined by integrating over the surface of the second. The force on the second piston per unit velocity of the first is called the mutual acoustic impedance. If the elements have an angular separation θ, the expression for the mutual impedance is

$$Z = i\pi a^2 \rho c \sum_{n=0}^{\infty} \epsilon_n \frac{[P_{n-1}(\cos \alpha) - P_{n+1}(\cos \alpha)]^2}{2n+1} P_n(\cos \theta) \quad .(5\text{-}14)$$

For $\theta = 0$, this gives the self impedance of the piston.

6. THICK DOME MODEL

The mathematical model illustrated in Fig. 6-1 consists of an infinite length cylinder and concentric dome. A velocity distribution independent of the axial direction is specified on the active surface of the transducer. It is desired to find the resulting sound pressure field in the fluid in regions 1 and 3 of Fig. 6-1. The boundary value problem is a three region problem: two fluid regions and the elastic dome region.

The general solution to the scalar wave equation in region 1 is

$$P_1 = \sum_{n=0}^{\infty} [A_n H_n^1(kr) + B_n H_n^2(kr)]\cos n\theta, \qquad (6-1)$$

where A_n and B_n are constants to be determined by boundary conditions. Equation (6-1) involves only cosine terms as the problem to be analyzed will arbitrarily be made even about $\theta = 0°$.

In region 3 the second pressure field is

$$P_3 = \sum_{n=0}^{\infty} C_n H_n^1(kr)\cos n\theta. \qquad (6-2)$$

Equation (6-2) satisfies the Sommerfeld radiation condition, and C_n is a constant to be specified by the boundary conditions.

At the transducer-fluid interface, the radial component of the fluid velocity must equal the velocity of the transducer. The radial velocity of the transducer may be expanded in a Fourier series of the form.

$$v_r = \frac{1}{i\rho c} \sum_{n=0}^{\infty} \delta_n \cos n\theta \qquad (6-3)$$
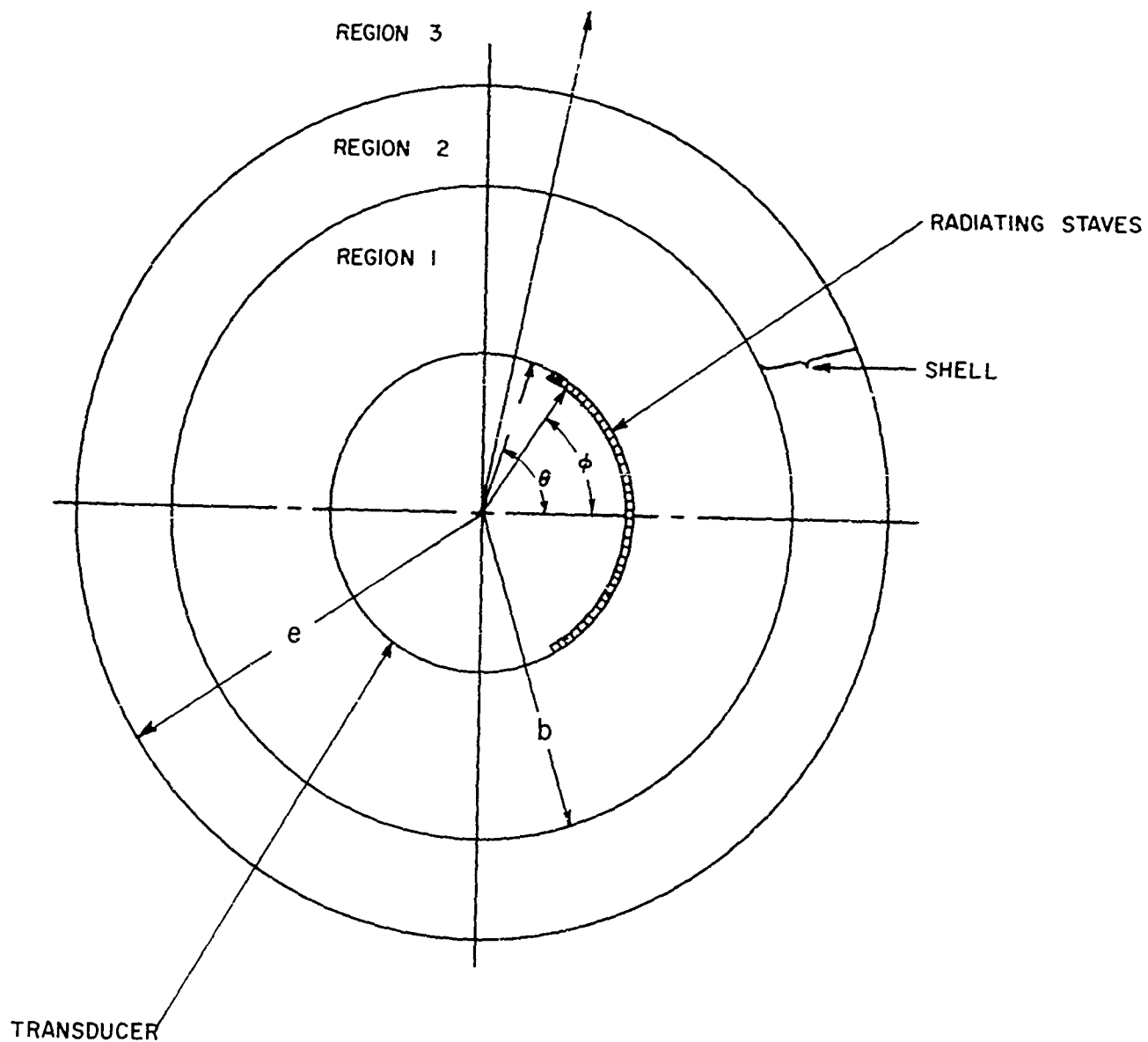
82

FIG. 6-1- PLAN FORM GEOMETRY FOR A CYLINDRICAL TRANSDUCER
RADIATING IN A THICK CONCENTRIC SHELL

83

The boundary condition at the transducer-fluid interface may now be matched to yield,

$$A_n H_n^{(1)'}(ka) + B_n H_n^{(2)'}(ka) = \delta_n , \qquad (6\text{-}4)$$

where the prime ($'$) denotes differentiation with respect to the argument of the Hankel function.

A means must now be devised to describe the motion of the thick shell. Let $\vec{v}$ be the velocity field vector of the thick shell, and $\vec{u}$ be the displacement field vector of the shell. Assume $\vec{u}$ and $\vec{v}$ are harmonically time dependent. The velocity and displacement field vectors are related as follows:

$$\vec{v} = -i\omega\vec{u} . \qquad (6\text{-}5)$$

An important property of a vector is that it may be represented as the gradient of a scalar plus the curl of a vector[11]. The vector $\vec{v}$ may be written as

$$\vec{v} = \vec{\nabla}\varphi + \vec{\nabla} \times \vec{\psi} . \qquad (6\text{-}6)$$

For this two-dimensional problem, $\vec{\psi} = \psi\vec{k}$. Both φ and ψ satisfy the scalar Helmholtz equation, while $\vec{v}$ is a solution of the vector Helmholtz equation[12]. The assumed solution forms for φ and ψ must satisfy the Helmholtz equation; and because the problem under consideration was assumed even, the solution forms must yield a radial velocity component which is an even function of θ and a tangential velocity component which is an odd function of θ. If the following forms are assumed for φ and ψ,

84

$$\varphi = \sum_{n=0}^{\infty} [D_n H_n^{(1)}(\zeta r) + E_n H_n^{(2)}(\zeta r)] \cos n\theta , \qquad (6\text{-}7)$$

$$\psi = \sum_{n=0}^{\infty} [F_n H_n^{(1)}(\xi r) + G_n H_n^{(2)}(\xi r)] \sin n\theta , \qquad (6\text{-}8)$$

then φ and ψ satisfy the scalar Helmholtz equation and meet the above requirements on the radial and tangential velocity components. The unknown coefficients D_n, E_n, F_n, and G_n will be determined so that the boundary conditions at both shell-fluid interfaces are satisfied. The quantities, $\zeta = \omega/c'$ and $\xi = \omega/c''$, are respectively the wave numbers associated with the compressional and shear waves in the dome. The compressional wave velocity is given by $c' = \sqrt{\dfrac{\lambda + 2\mu}{\rho_s}}$, and the shear wave velocity is given by $c'' = \sqrt{\dfrac{\mu}{\rho_s}}$. In the velocity expressions, λ and μ are the Lame constants, and ρ_s is the density of the shell [13].

From Eqs. (6-5) and (6-6) one finds that

$$\vec{u} = \frac{i}{\omega} [\vec{\nabla}\varphi + \vec{\nabla} \times \vec{\psi}] , \qquad (6\text{-}9)$$

where

$$\vec{\nabla} = \vec{e}_r \frac{\partial}{\partial r} + \vec{e}_\theta \frac{1}{r} \frac{\partial}{\partial \theta} . \qquad (6\text{-}10)$$

The unit vector in the radial direction is $\vec{e}_r$ and in the tangential direction $\vec{e}_\theta$. If Eqs. (6-7)-(6-10) are combined, the results are

$$u_\theta = \frac{-i}{\omega} \sum_{n=0}^{\infty} [\frac{n}{r}\{D_n H_n^{(1)}(\zeta r) + E_n H_n^{(2)}(\zeta r)\} + \xi\{F_n H_n^{(1)\prime}(\xi r) + G_n H_n^{(2)\prime}(\xi r)\}] \sin n\theta ,$$
$$(6\text{-}11)$$

$$u_r = \frac{i}{\cdot} \sum_{n=0}^{\infty} \, \left\{ D_n H_n^{(1)\prime}(\varsigma r) + E_n H_n^{(2)\prime}(\varsigma r) \right\} + \frac{n}{r} \left\{ F_n H_n^{(1)}(\xi r) + G_n H_n^{(2)}(\xi r) \right\} \, \right] \cos n\theta ,$$
$$(6-12)$$

where u_θ is the displacement of the shell in the tangential direction and u_r is the displacement of the shell in the radial direction.

The boundary conditions which must be satisfied at the inner and outer surfaces of the thick shell are

$$S_{rr}\Big]_{r=b} = - P_1 \quad , \tag{6-13}$$

$$S_{rr}\Big]_{r=e} = - P_3 \quad , \tag{6-14}$$

$$S_{r\theta}\Big]_{r=b} = 0 \quad , \tag{6-15}$$

$$S_{r\theta}\Big]_{r=e} = 0 \quad , \tag{6-16}$$

where the radial stress in the shell is denoted by S_{rr} and the tangential stress by $S_{r\theta}$. In addition to Eqs. (6-13) - (6-16), there is another requirement that the velocity of the shell at the radii $r = b$ and $r = e$ must equal the velocity of the fluid at $r = b$ and $r = e$.

The equations relating stress and displacement components are

$$S_{rr} = (\lambda + 2\mu) \frac{\partial u_r}{\partial r} + \frac{\lambda}{r} \left[u_r + \frac{\partial u_\theta}{\partial \theta} \right] , \tag{6-17}$$

86

and

$$S_{r\theta} = \mu \left[\frac{1}{r} \frac{\partial u_r}{\partial \theta} + \frac{\partial u_\theta}{\partial r} - \frac{1}{r} u_\theta \right] . \qquad (6\text{-}18)$$

To obtain the stress relations in terms of the unknown coefficients D_n, E_n, etc., one substitutes Eqs. (6-11) and (6-12) into Eqs. (6-17) and (6-18) to obtain Eqs. (6-20) and (6-21) in Table 6-I. It is now possible to satisfy the boundary conditions specified by Eqs. (6-13) and (6-12) to obtain Eqs. (6-21) and (6-22) in Table 6-I. When Eqs. (6-15) and (6-16) are satisfied, the results are Eqs. (6-23) and (6-24) in Table 6-I.

The two remaining boundary conditions which must be met are the velocity conditions at the shell-fluid interfaces. If the velocity boundary conditions at the shell-fluid interfaces are matched, and the unknown coefficient B_n is eliminated by use of Eq. (6-4), the results are Eqs. (6-25) and (6-26) in Table 6-I.

The quantity δ_n which appears in Eqs. (6-3) and (6-25) may be computed from the velocity prescription on the transducer [7]. Equations (6-21) - (6-26) fully describe the problem under consideration. These may be solved for the unknown coefficients A_n, C_n, D_n, E_n, F_n, and G_n.

With all unknown coefficients determined, the pressure fields in the fluid are determined by Eqs. (6-1) and (6-2).

Table 6-I
EQUATIONS FOR THICK DOME MODEL

(6-19)
$$S_{rr} = \frac{i}{r}\left\{\sum_{n=0}^{\infty} D_n [(\lambda+2\mu)\zeta^2 H_n^{(1)''}(\zeta r) + \frac{\lambda\zeta}{r} H_n^{(1)'}(\zeta r) - \frac{\lambda n^2}{r} H_n^{(1)}(\zeta r)] + \right.$$

$$E_n [(\lambda+2\mu)\zeta^2 H_n^{(2)''}(\zeta r) + \frac{\lambda\zeta}{r} H_n^{(2)'}(\zeta r) - \frac{\lambda n^2}{r} H_n^{(2)}(\zeta r)] +$$

$$F_n \frac{2\mu n}{r}[\xi H_n^{(1)'}(\xi r) - \frac{1}{r} H_n^{(1)}(\xi r)] +$$

$$\left. G_n \frac{2\mu n}{r}[\xi H_n^{(2)'}(\xi r) - \frac{1}{r} H_n^{(2)}(\xi r)]\right\} \cos n\theta .$$

(6-20)
$$S_{r\theta} = \frac{-i\mu}{r}\left\{\sum_{n=0}^{\infty} D_n \frac{2n}{r}[\zeta H_n^{(1)'}(\zeta r) - \frac{1}{r} H_n^{(1)}(\zeta r)] + \right.$$

$$E_n \frac{2n}{r}[\zeta H_n^{(2)'}(\zeta r) - \frac{1}{r} H_n^{(2)}(\zeta r)] +$$

$$F_n[\xi^2 H_n^{(1)''}(\xi r) - \frac{\xi}{r} H_n^{(1)'}(\xi r) + \frac{n^2}{r^2} H_n^{(1)}(\xi r)] +$$

$$\left. G_n[\xi^2 H_n^{(2)''}(\xi r) - \frac{\xi}{r} H_n^{(2)'}(\xi r) + \frac{n^2}{r^2} H_n^{(2)}(\xi r)]\right\} \sin n\theta .$$

(6-21)
$$D_n[(\lambda + 2\mu)\zeta^2 H_n^{(1)''}(\zeta b) + \frac{\lambda\zeta}{b} H_n^{(1)'}(\zeta b) - \frac{\lambda n^2}{b^2} H_n^{(1)}(\zeta b)] +$$

$$E_n[(\lambda + 2\mu)\zeta^2 H_n^{(2)''}(\zeta b) + \frac{\lambda\zeta}{b} H_n^{(2)'}(\zeta b) - \frac{\lambda n^2}{b^2} H_n^{(2)}(\zeta b)] +$$

$$F_n \frac{2\mu n}{b}[\xi H_n^{(1)'}(\xi b) - \frac{1}{b} H_n^{(1)}(\xi b)] +$$

$$G_n \frac{2\mu n}{b}[\xi H_n^{(2)'}(\xi b) - \frac{1}{b} H_n^{(2)}(\xi b)] = i\omega[A_n H_n^{(1)}(kb) + B_n H_n^{(2)}(kb)] .$$

88

Table 6-I(con't)

(6-22)
$$D_n [(\lambda + 2\mu) \zeta^2 H_n^{(1)''}(\zeta e) + \frac{\lambda \zeta}{e} H_n^{(1)'}(\zeta e) - \frac{\lambda n^2}{e^2} H_n^{(1)}(\zeta e)] +$$

$$E_n [(\lambda + 2\mu) \zeta^2 H_n^{(2)''}(\zeta e) + \frac{\lambda \zeta}{e} H_n^{(2)'}(\zeta e) - \frac{\lambda n^2}{e^2} H_n^{(2)}(\zeta e)] +$$

$$F_n \frac{2\mu n}{e} [\xi H_n^{(1)'}(\xi e) - \frac{1}{e} H_n^{(1)}(\xi e)] +$$

$$G_n \frac{2\mu n}{e} [\xi H_n^{(2)'}(\xi e) - \frac{1}{e} H_n^{(2)}(\xi e)] =$$

$$i \omega c_n H_n^{(1)}(ke)$$

(6-23)
$$D_n [H_n^{(1)'}(\zeta b) - \frac{1}{b} H_n^{(1)}(\zeta b)] \frac{2n}{b} + E_n [H_n^{(2)'}(\zeta b) - \frac{1}{b} H_n^{(2)}(\zeta b)] \frac{2n}{b} +$$

$$F_n [\xi^2 H_n^{(1)''}(\xi b) - \frac{\xi}{b} H_n^{(1)'}(\xi b) + \frac{n^2}{b^2} H_n^{(1)}(\xi b)] +$$

$$G_n [\xi^2 H_n^{(2)''}(\xi b) - \frac{\xi}{b} H_n^{(2)'}(\xi b) + \frac{n^2}{b^2} H_n^{(2)}(\xi b)] = 0$$

(6-24)
$$D_n [H_n^{(1)'}(\zeta e) - \frac{1}{e} H_n^{(1)}(\zeta e)] \frac{2n}{e} + E_n [H_n^{(2)'}(\zeta e) - \frac{1}{e} H_n^{(2)}(\zeta e)] \frac{2n}{e} +$$

$$F_n [\xi^2 H_n^{(1)''}(\xi e) - \frac{\xi}{e} H_n^{(1)'}(\xi e) + \frac{n^2}{e^2} H_n^{(1)}(\xi e)] +$$

$$G_n [\xi^2 H_n^{(2)''}(\xi e) - \frac{\xi}{e} H_n^{(2)'}(\xi e) + \frac{n^2}{e^2} H_n^{(2)}(\xi e)] = 0 .$$

89

Table 6-I (cont'd)

(6-25)
$$D_n \, i \, c\rho\varsigma \, H_n^{(1)\prime}(\varsigma b) + E_n \, i \, c\rho\varsigma \, H_n^{(2)\prime}(\varsigma b) + i \, c\rho\frac{n}{b} F_n \, H_n^{(1)}(\xi b) +$$

$$G_n \, \frac{i \, c\rho n}{b} H_n^{(2)}(\xi b) - A_n \left[H_n^{(1)\prime}(kb) - \frac{H_n^{(2)\prime}(kb) \, H_n^{(1)\prime}(ka)}{H_n^{(2)\prime}(ka)} \right] =$$

$$\frac{H_n^{(2)\prime}(kb)}{H_n^{(2)\prime}(ka)} \, \delta_n \quad .$$

(6-26)
$$D_n \, i \, c\rho\varsigma \, H_n^{(1)\prime}(\varsigma e) + E_n \, i \, c\rho\varsigma \, H_n^{(2)\prime}(\varsigma e) + F_n \, \frac{i \, c\rho n}{e} H_n^{(1)}(\xi e) +$$

$$G_n \, \frac{i \, c\rho n}{e} H_n^{(2)}(\xi e) - C_n \, H_n^{(1)\prime}(ke) = 0 \quad .$$

90

7. STRUCTURE MODEL

The solution to the problem of a cylindrical transducer mounted inside a concentric, homogeneous, cylindrical dome has been reported previously [7]. The mathematical model considered in this section extends the solution to that problem by incorporating dome structure into the mathematical model.

The model shown in Fig. 7-1 consists of an infinite cylindrical transducer enclosed by a concentric cylindrical shell. At locations where structure elements are attached to the shell there is added impedance to the shell motion. In the present analysis this impedance is assumed to be mass-like, although the analysis is easily extended to include a more complicated type of impedance. In the analysis of the shell, the structure mass contribution is included by inserting an inertial load, or D'Alembert force, in the Flügge shell equations.

Flügge's shell equations written in terms of displacements of the middle surface are:

$$\frac{\partial^2 u_\theta}{\partial \theta^2} + \frac{\partial u_r}{\partial \theta} + P_\theta \frac{b^2}{E_s h} = 0 , \qquad (7-1)$$

$$\frac{\partial u_\theta}{\partial \theta} + u_r + \frac{h^2}{12 b^2} \left[\frac{\partial^4 u_r}{\partial \theta^4} + 2 \frac{\partial^2 u_r}{\partial \theta^2} + u_r \right] - P_r \frac{b^2}{E_s h} = 0 . \quad (7-2)$$

The radial and tangential displacements are respectively u_r and u_θ. The tangential and radial force components acting on the system are P_θ and P_r, respectively, while $E_s = \frac{E}{1-\nu^2}$, b is the radius of the middle surface of the dome, h is the thickness of the dome, and ν is Poisson's ratio. Equations (7-1) and
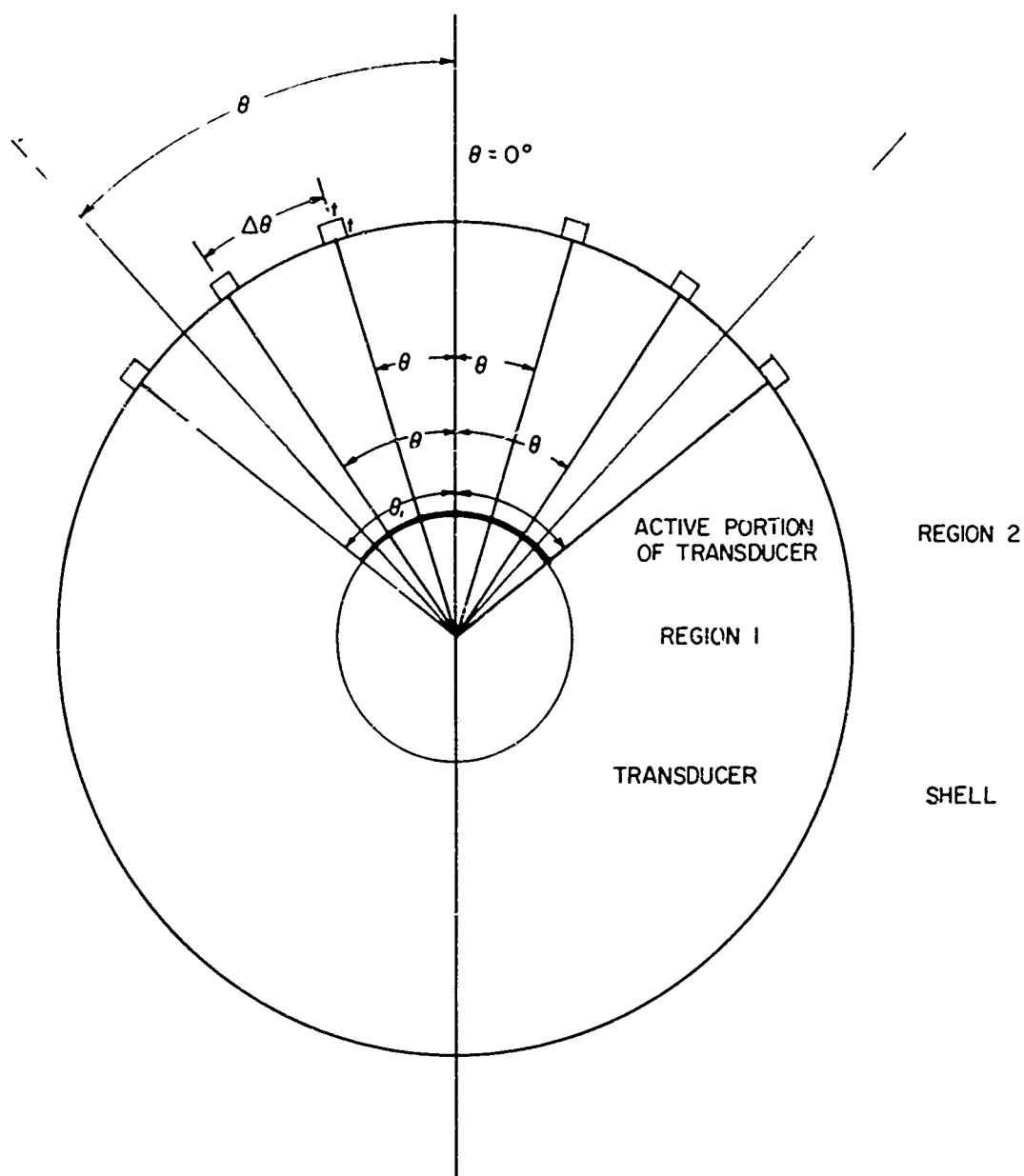
FIG. 7-1 - PLAN FORM GEOMETRY FOR A CYLINDRICAL TRANSDUCER RADIATING IN A CONCENTRIC NON-HOMOGENEOUS SHELL

(7-2) are static equations but may be converted to dynamic equations by including an additional D'Alembert force. Since the fluid is assumed to be inviscid, there is no tangential force acting on the shell. Equations (7-1) and (7-2) become respectively,

$$\omega^2 \sigma u_\theta + \frac{E_s h}{b^2}\left[\frac{\partial u_\theta^2}{\partial \theta^2} + \frac{\partial u_r}{\partial \theta}\right] = 0 \quad , \tag{7-3}$$

$$-\omega^2 \sigma u_r + \frac{E_s h}{b^2}\left[\frac{\partial u_\theta}{\partial \theta} + u_r\right] + \frac{E_s h^3}{12b^4}\left[\frac{\partial^4 u_r}{\partial \theta^4} + \frac{2d^2 u_r}{\partial \theta^2} + u_r\right] = P_1 - P_2 . \tag{7-4}$$

The quantity σ is the surface density of the dome, and P_1 and P_2 are the acoustic pressures in regions 1 and 2, respectively.

The surface density of the dome, σ, must be expressed in a manner that accounts for surface density discontinuities at structure locations. The surface density of the dome can be written

$$\sigma = \rho_s h + \frac{M\delta(\theta) t}{A} \quad , \tag{7-5}$$

where ρ_s is density of dome, h is thickness of dome, M is mass per unit length of structure element, t is thickness of structure, A is cross-sectional area of structure element, and

$$\delta(\theta) = \begin{cases} 0 & \theta > (\theta_j + \xi) \\ 1 & (\theta_j - \xi) < \theta < (\theta_j + \xi) \\ 0 & \theta < (\theta_j - \xi) \end{cases} \quad . \tag{7-6}$$

93

One additional assumption is that the structure element does not affect the tangential D'Alembert force.

The radial and tangential velocity components of the dome are given by $W = \frac{\partial u_r}{\partial t} = -i r u_r$, and $V = \frac{\partial u_\theta}{\partial t} = i r u_\Omega$, respectively, for harmonic time dependence. When the above are substituted into Eqs. (7-3) and (7-4), the results are

$$r^2 \rho_s h V + \frac{E_s h}{b^2}\left[\frac{\partial^2 V}{\partial \theta^2} + \frac{\partial W}{\partial \theta}\right] = 0 \quad , \tag{7-7}$$

$$-r^2 \rho_s h W - r^2 \frac{M}{A} \delta(\theta)\, tW + \frac{E_s h}{b^2}\left[\frac{\partial V}{\partial \theta} + W\right] + \frac{E_s h^3}{12 b^4}\left[\frac{\partial^4 W}{\partial \theta^4} + \frac{2\partial^2 W}{\partial \theta^2} + W\right]$$

$$= -i\omega[P_1 - P_2] \quad . \tag{7-8}$$

The velocity components, V and W, are the total velocity components of the dome as are the pressure fields P_1 and P_2. Assume that the total velocity components and pressure fields may be written in two parts:

$$V = v + \bar{v} \quad , \tag{7-9}$$

$$W = w + \bar{w} \quad , \tag{7-10}$$

$$P_1 = p_1 + \bar{p}_1 \quad , \tag{7-11}$$

$$P_2 = p_2 + \bar{p}_2 \quad . \tag{7-12}$$

The unbarred quantities are the non-structure components, and the barred quantities are the components due to the presence of structure. If Eqs. (7-9) - (7-12) are substituted into Eqs. (7-7) and (7-8), and if the non-structure solution to the problem is subtracted from these results, the resulting equations are,

94

$$\omega^2 \rho_s h \, \bar{v} + \frac{E_s h}{b^2}\left[\frac{\partial^2 \bar{v}}{\partial \theta^2} + \frac{\partial \bar{w}}{\partial \theta}\right] = 0 \ , \tag{7-13}$$

$$-\omega^2 \rho_s h \, \bar{w} - \omega^2 \frac{M}{A} \delta(\theta) t \, (w + \bar{w}) + \frac{E_s h}{b^2}\left[\frac{\partial \bar{v}}{\partial \theta} + \bar{w}\right] +$$

$$\frac{E_s h^3}{12 b^4}\left[\frac{\partial^4 \bar{w}}{\partial \theta^4} + \frac{2\partial^2 \bar{w}}{\partial \theta^2} + \bar{w}\right] = -i\omega \, [\bar{p}_1 - \bar{p}_2] \ . \tag{7-14}$$

For an even problem, the quantities $\bar{w}$, $\bar{v}$, $\bar{v}$, and $\bar{p}_1$, and $\bar{p}_2$ may be expressed by the following Fourier series:

$$\bar{v} = \sum_{n=0}^{\infty} \bar{D}_n \sin n\theta \ , \tag{7-15}$$

$$\bar{w} = \sum_{n=0}^{\infty} \bar{G}_n \cos n\theta \ , \tag{7-16}$$

$$\bar{p}_1 = \sum_{n=0}^{\infty} [\bar{A}_n J_n(kr) + \bar{B}_n N_n(kr)] \cos n\theta \ , \tag{7-17}$$

$$\bar{p}_2 = \sum_{n=0}^{\infty} \bar{C}_n H_n^{(1)}(kr) \cos n\theta \ . \tag{7-18}$$

When Eqs. (7-15) - (7-18) are substituted into Eqs. (7-13) and (7-14), and the orthogonality properties of the sine functions are employed, the results are

$$\left[\omega^2 \rho_s - \frac{E_s}{b^2} n^2\right] \bar{D}_n - \frac{E_s n}{b^2} \bar{G}_n = 0, \tag{7-19}$$

95

$$-\omega^2 \rho_s h \bar{G}_n \frac{2\pi}{\varepsilon_n} - M\omega^2 t \int_{-\pi}^{\pi} \frac{\delta(\cdot\cdot)}{A}(w + \bar{w})\cos n\theta \, d\theta + \frac{E_s h}{b^2}[n \bar{D}_n + \bar{G}_n] \frac{2\pi}{\varepsilon_n}$$

$$+ \frac{E_s h^3}{12b^4} \frac{2\pi}{\varepsilon_n}[n^4 \bar{G}_n - 2n^2 \bar{G}_n + \bar{G}_n] = -i\omega\frac{2\pi}{\varepsilon_n}[\bar{A}_n J_n(kb) + \bar{B}_n N_n(kb)] + i\omega\frac{2\pi}{\varepsilon_n}\bar{C}_n H_n^{(1)}(kb).$$

$$(7\text{-}20)$$

Equation (7-16), along with the fact that the structure angular half-width (ξ) may be taken as small as desired, allows the integral, I, in Eq. (7-20) to be evaluated with the following results:

$$I = -\frac{M\omega^2}{b} \sum_{j=1}^{jmax} \frac{1}{n\xi} (w + \bar{w})_{\theta=\theta_j} \cos n\theta_j \sin n\xi. \qquad (7\text{-}21)$$

Equation (7-21) when substituted in Eq. (7-20) yields

$$- i\omega \bar{A}_n J_n(kb) - i\omega \bar{B}_n N_n(kb) + i\omega \bar{C}_n H_n^{(1)}(kb) - \frac{E_s hn}{b^2} \bar{D}_n +$$

$$h \left\{ \omega^2 \rho_s - \frac{E_s}{b^2}[1 + \frac{h^2}{12b^2}(n^4 - 2n^2 + 1)]\right\} \bar{G}_n + \frac{M\omega^2}{b} \sum_{j=1}^{jmax} \frac{1}{n\xi}(w+\bar{w})_{\theta=\theta_j}\frac{\varepsilon_n}{2\pi} \times$$

$$(7\text{-}22)$$

$$\cos n\theta_j \sin n\xi = 0.$$

Boundary conditions on the surface of the transducer must be matched. It is important to realize that the velocity prescription of the transducer face has not been changed by the addition of the rib structure to the dome. The boundary condition at the transducer face is

$$\left.\frac{\partial P_1}{\partial r}\right|_{r=a} = v_t \quad, \qquad (7\text{-}23)$$

96

$$\frac{\partial (p_1 + \bar{p}_1)}{\partial r}\bigg|_{r=a} = v_t \quad . \tag{7-24}$$

When the non-structure result is subtracted from Eq. (7-24), the condition to be met is that

$$\frac{\partial \bar{p}_1}{\partial r}\bigg|_{r=a} = 0 \quad , \tag{7-25}$$

$$\bar{A}_n J_n'(ka) + \bar{B}_n N_n'(ka) = 0 \quad . \tag{7-26}$$

The velocity boundary conditions at the dome-fluid interface are

$$\frac{\partial P_2}{\partial r}\bigg|_{r=b} = i\omega\rho W\bigg|_{r=b} \quad , \tag{7-27}$$

$$\frac{\partial P_1}{\partial r}\bigg|_{r=b} = i\omega o W\bigg|_{r=b} \quad . \tag{7-28}$$

When Eqs. (7-15) - (7-18) are substituted in Eqs. (7-27) and (7-28), the results of matching boundary conditions at the dome-fluid interface yield the following relations,

$$\bar{A}_n J_n'(kb) + \bar{B}_n N_n'(kb) - ic\rho \, \bar{G}_n = 0 \quad , \tag{7-29}$$

$$\bar{C}_n H_n^{(1)}{}'(kb) - ic\rho \, \bar{G}_n = 0 \quad . \tag{7-30}$$

In Eq. (7-16) it was assumed that $\bar{w}$ could be written as a Fourier series. Equations (7-19), (7-26), (7-29), and (7-30) allow Eq. (7-22) to be written in terms of only one unknown

97

coefficient, namely $\bar{G}_n$. The form of $\bar{G}_n$ in Eq. (7-16) may now be specified as

$$\bar{G}_n = \phi_n \frac{M\omega^2}{b} \sum_{j=1}^{jmax} \frac{1}{n\xi} (w + \bar{w})_{\theta=\theta_j} \frac{\epsilon_n}{2\pi} \cos n\theta_j \sin n\xi \ , \quad (7\text{-}31)$$

where

$$\phi_n = \left\{ \frac{-1}{\left[\frac{rc\rho [J_n(kb)N_n'(ka)-N_n(kb)J_n'(ka)]}{J_n'(kb)N_n'(ka)-N_n'(kb)J_n'(ka)} - \frac{\omega c\rho H_n(kb)}{H_n'(kb)} + h\left[\omega^2 \rho_s \right.\right.} \right.$$
$$\left. \left. - \frac{E_s}{b^2}\left[1 + \frac{h^2}{12b^2}(n^4-2n^2+1)\right] - \frac{E_s^2 n^2}{b^2(\omega^2\rho_s b^2 - E_s n^2)}\right] \right\} .$$

If Eq. (7-31) is substituted in Eq. (7-16) and $\bar{w}$ is evaluated at angles $\theta = \theta_k$, then $\bar{w}_{\theta k}$ is

$$\bar{w}_{\theta k} = \sum_{n=o}^{\infty} \frac{\epsilon_n}{2\pi} \frac{1}{n\xi} Z \phi_n \sin n\xi \sum_{j=1}^{jmax} (w + \bar{w})_{\theta_j} \cos n\theta_j \cos n\theta_k \ ,$$
$$(7\text{-}32)$$

where Z is the "structure coefficient" defined by $Z = \frac{M\omega^2}{b}$,

$$\bar{w}_k = \sum_{j=1}^{jmax} (w_{\theta_j} + \bar{w}_{\theta_j}) \psi_{jk} \ , \quad (7\text{-}33)$$

$$\psi_{jk} = \frac{Z}{2\pi\xi} \sum_{n=o}^{\infty} \frac{\epsilon_n \phi_n}{n} \sin n\xi \cos n\theta_j \cos n\theta_k \ , \quad (7\text{-}34)$$

98

$$\bar{w}_{\theta_k} = \sum_{j=1}^{jmax} w_{\theta_j} \, \psi_{jk} + \sum_{j=1}^{jmax} \bar{w}_{\theta_j} \, \psi_{jk} \, ,$$

$$\bar{w}_{\theta_k} = \sum_{j=1}^{jmax} \delta_{jk} \, \bar{w}_{\theta_k} \, ,$$

$$\delta_{ik} = \begin{Bmatrix} 0 & j \neq k \\ 1 & j = k \end{Bmatrix} \, .$$

The equation for $\bar{w}_{\theta_k}$ may be expressed in matrix form

$$\begin{bmatrix} (1 - \psi_{11}) & -\psi_{21} & - - - - - & \psi_{j_{max},1} \\ -\psi_{12} & (1 - \psi_{22}) & - - - - - & \psi_{j_{max},2} \\ \vdots & - - - - - - - - - - - & \\ \psi_{1,kmax} & -\psi_{2,kmax} & - - - & (1 - \psi_{j_{max},kmax}) \end{bmatrix} \begin{bmatrix} \bar{w}_{\theta_1} \\ \bar{w}_{\theta_2} \\ - - \\ \bar{w}_{\theta_{kmax}} \end{bmatrix} = \begin{bmatrix} \sum_{j=1}^{jmax} w_{\theta_j} \psi_{j,1} \\ \sum_{j=1}^{jmax} w_{\theta_j} \psi_{j,2} \\ - - - - \\ \sum_{j=1}^{jmax} w_{\theta_j} \psi_{j,kmax} \end{bmatrix} \, ,$$

$$(7\text{-}35)$$

and the matrix may be inverted by standard inversion techniques. With the velocity components $\bar{w}_{\theta_k}$ known, the coefficient $\bar{G}_n$ may be determined by Eq. (7-31) and, in turn, all other unknown coefficients, $\bar{D}_n$, $\bar{A}_n$, $\bar{B}_n$, and $\bar{C}_n$ can be determined. This allows computation of the pressure fields in regions 1 and 2, thus completing the solution.

8. INFINITE PLANAR MODEL

The infinite planar dome-transducer model is shown in Fig. 8-1, along with the coordinate geometry. A thin plate is located a distance d from the planar "transducer." The transducer surface has a continuous normal velocity distribution which simulates the particle velocity of a plane wave traveling in a direction making an angle θ with the normal to the plane. This velocity distribution is given by

$$V = V_o e^{ik \, x \, \sin\theta} \,, \tag{8-1}$$

where V_o is just a velocity amplitude factor. The pressure field between the dome and transducer will be denoted by p_1, and that outside the dome by p_2. In order for the fluid particle velocity to equal the transducer velocity at $y = 0$,

$$\frac{1}{i\omega\rho} \frac{\partial p}{\partial y}\bigg|_{y=0} = V. \tag{8-2}$$

The plate is assumed to be thin enough that the boundary conditions at its surfaces may be matched at the middle surface. One condition is that the fluid particle velocity at the inner and outer plate surfaces equal the plate velocity. If the plate displacement from equilibrium is denoted by u, the equality of velocities is given by

$$\frac{1}{i\omega\rho}\left[\frac{\partial p}{\partial y}\right]_{y=d} = \frac{1}{i\omega\rho}\left[\frac{\partial p_2}{\partial y}\right]_{y=d} = \frac{\partial u}{\partial t} \,. \tag{8-3}$$

100

TRANSMITTED WAVE DIRECTION

REFLECTED WAVE
DIRECTION

ELASTIC PLANAR DOME

d, dome transducer spacing

θ

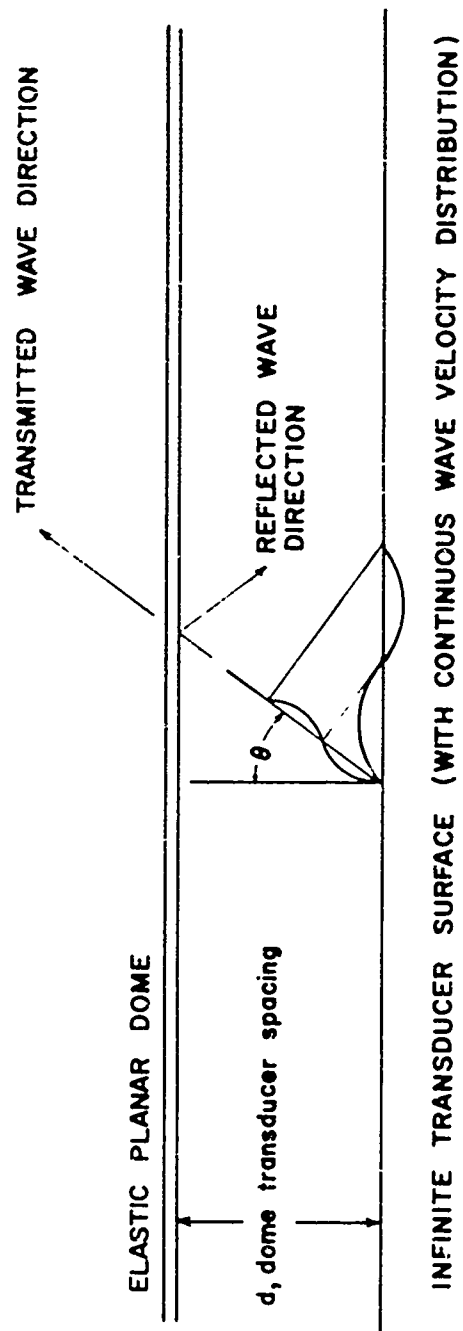INFINITE TRANSDUCER SURFACE (WITH CONTINUOUS WAVE VELOCITY DISTRIBUTION)

FIG. 8-1 - GEOMETRY OF INFINITE PLANAR DOME — TRANSDUCER MODEL

The dynamic behavior of the plate is described by the classical plate equation. In this case the driving force is the pressure difference across the plate, so the equation takes the form

$$\left[P_1 - P_2 \right]_{y=d} = \rho_s h \frac{\partial^2 u}{\partial t^2} + \frac{Eh^3}{12(1-\nu^2)} \frac{\partial^4 u}{\partial x^4} \ . \tag{8-4}$$

Here ρ_s is the plate mass density, h is its thickness, E is Young's modulus, and ν is Poisson's ratio.

The solutions to the wave equation for the pressure fields inside and outside of the dome will have the forms

$$P_1 = \left[A\, e^{i\eta y} + B\, e^{-i\eta y} \right] e^{iKx} \ , \quad \eta^2 + K^2 = k^2 \tag{8-5}$$

$$P_2 = C\, e^{i\eta y}\, e^{iKx} \ . \tag{8-6}$$

Substituting these equations into the boundary condition equations yields expressions for the unknown coefficients in Eqs. (8-4) and (8-5). The final results for the pressure fields are

$$P_1 = \frac{i \rho c\, V_o}{D} \left[e^{i\eta(y-d)} + \frac{i\eta}{x^2 \rho}(-\sigma \omega^2 + HK^4)\, \cos\, \eta(y-d) \right] e^{iKx} \tag{8-7}$$

$$P_2 = \frac{i \rho c\, V_o}{D}\, e^{i\eta(y-d)}\, e^{iKx} \ . \tag{8-8}$$

where $\sigma = \rho_s h$, $H = \dfrac{Eh^3}{12(1-\nu^2)}$, $K = k \sin\theta$, $\eta = k \cos\theta$

$$D = i\eta \left\{ e^{-i\eta d} + \frac{\eta}{x^2 \rho}(-\sigma\omega^2 + HK^4)\, \sin\, \eta d \right\} \ .$$

It is seen that p_1 is the sum of the traveling wave which is transmitted through the dome and a standing wave which always has an

antinode at the plate. The average intensity passing through
the plate is just

$$I_o = \frac{1}{2cc} \frac{(\pi c V_o)^2}{|D|^2} \quad . \tag{8-9}$$

For many cases of interest the HK^4 term in Eq. (8-8) is
small relative to the $\sigma \omega^2$, and, in this case

$$D \approx i\pi \{e^{-i\pi d} - h \frac{c_s}{c} \pi \sin \pi d\}.$$

Defining R as the ratio of D in Eq. (8-9) to the value of I_o would
have with no dome, h = 0, gives

$$R = 1/\{1 + \pi h \frac{c_s}{\rho} \sin \pi d [\pi h \frac{\rho_s}{\rho} \sin \pi d - 2 \cos \pi d]\}. \tag{8-10}$$

It is seen that R is a periodic function of d, with period
$\pi/k \cos\theta$, and that its amplitude of oscillation decreases as
θ increases. Starting from d = 0, R increases from unity until
its first maximum occurs at a value of d for which

$$\tan 2 \pi d = 2 \pi h \rho_s/c \quad . \tag{8-11}$$

Typically, $\rho_s/\rho \approx 7.9$ and $kh \approx 1.8 \times 10^{-2}$, so for $\theta = 0$, tan 2 πd =
0.284. For this small value, tan 2 $\pi d \sim 0.14$. This is a plate-
transducer spacing of 0.023 wavelengths. Maxima occur at this
value of d and at every half wavelength thereafter.

REFERENCES

1. Radiation Characteristics of a Circular Transducer Surrounded by a Nonconcentric Circular Shell, TRACOR Document No. 66-579-U, October 11, 1966.

2. Morse and Feshbach, _Methods of Theoretical Physics_, McGraw-Hill, New York, 1953, Chap. 13.

3. Analytical Studies of Dome-Transducer Interactions, TRACOR Document No. 66-342-U, June 9, 1966.

4. O. D. Kellogg, _Foundations of Potential Theory_, Dover, New York, 1953, Chap. 6.

5. _Handbook of Mathematical Functions_, NBS Applied Math Series-55, pp. 369-370, June 1964.

6. C. Lanczos, _Linear Differential Operators_, D. Van Nostrand, New York, 1964, Chap. 1.

7. An Improved Analytical Model of the Interaction of Domes and Transducers During Transmission, TRACOR Document No. 65-292-U, August 31, 1965.

8. W. Flügge, _Stresses in Shells_, Springer-Verlog, Berlin, 1962, p. 219.

9. Mathews and Walker, _Mathematical Methods of Physics_, W. A. Benjamin, Inc., New York, 1965, p. 78.

10. Radiation Characteristics of a Spherical Transducer Surrounded by a Concentric Shell, TRACOR Document No. 67-178-U, February 10, 1967.

11. H. Lass, _Vector and Tensor Analysis_, McGraw-Hill, New York, 1950, p. 157.

12. Morse and Feshbach, Methods of Theoretical Physics, McGraw-Hill, New York, 1953, p. 1772.

13. I. S. Sokolnikoff, Mathematical Theory of Elasticity, McGraw-Hill, New York, 1956, p. 68.